Copyright Warning & Restrictions

The copyright law of the United States (Title 17, United States Code) governs the making of photocopies or other reproductions of copyrighted material.

Under certain conditions specified in the law, libraries and archives are authorized to furnish a photocopy or other reproduction. One of these specified conditions is that the photocopy or reproduction is not to be "used for any purpose other than private study, scholarship, or research." If a, user makes a request for, or later uses, a photocopy or reproduction for purposes in excess of "fair use" that user may be liable for copyright infringement,

This institution reserves the right to refuse to accept a copying order if, in its judgment, fulfillment of the order would involve violation of copyright law.

Please Note: The author retains the copyright while the New Jersey Institute of Technology reserves the right to distribute this thesis or dissertation

Printing note: If you do not wish to print this page, then select "Pages from: first page # to: last page #" on the print dialog screen

ABSTRACT

ENHANCED MEMBRANE DISTILLATION: ANALYTICAL AND DEIONIZATION APPLICATIONS

By

Ken Gethard

Membrane distillation (MD) is a newer technology that is being investigated for applications such as seawater desalination and concentration of fruit and sucrose solutions. The major advantage of MD over traditional thermal distillation is that it requires a substantially lower thermal energy requirement to power the process. This allows low grade energy sources such as waste heat or solar energy to be used with MD. Compared to concentration processes such as reversed osmosis or ion-exchange, MD does not require specialized equipment, high electrical consumption, the use of strong acids and bases nor does it generate hazardous waste as a by-product.

In membrane distillation, a heated solution is passed through the lumen of a hollow fiber porous hydrophobic membrane. The vapor pressure differential between the cool and hot side of the membrane allows the vapor to pass across the pores but prevents passage of the liquid phase. Unlike pervaporation, which also relies on differential vapor pressure, MD also involves the transfer of a significant amount of heat across the membrane. MD processes to date have demonstrated several inefficiencies that cause it to be a relatively low yield process. These inefficiencies include conductive heat loss through the membrane material, temperature polarization at the bulk feed-membrane interface, pore wetting and effective use of available membrane surface area.

In this investigation, traditional membrane distillation was compared to membrane distillation using the same starting membrane material but which had carbon nanotubes (CNTs) incorporated into the membrane pores. The modified membrane is referred to as carbon nanotube immobilized membrane (CNIM). It was demonstrated that several properties of CNTs aided in improving the performance of MD. These include high thermal conductance, rapid sorption-desorption ability, ability to transport water in a rapid ordered manner and hydrophobic characteristics.

Experiments were conducted where MD was used as a preconcentration technique to analyze trace quantities of drug substance in water. CNIM provided much higher levels of enrichment for the analytes of interest than did preconcentration using the plain membrane. Another set of experiments was then successfully conducted that demonstrated that CNIM-MD was applicable to the preconcentration of drug products in a polar solvent. Desalination experiments were completed that showed that CNIM provided significantly higher levels of salt reduction and flux at a lower energy requirement than did the standard membrane. Finally, MD-CNIM was investigated as a means to remove or concentrate trace levels of inorganic impurities from an aqueous matrix.

Overall, it was demonstrated that MD using CNIM provided a more efficient process with significantly higher solvent reduction and levels of enrichment than did MD using plain membranes.

ENHANCED MEMBRANE DISTILLATION: ANALYTICAL AND DEIONIZATION APPLICATIONS

by
Ken Gethard

A Dissertation
Submitted to the Faculty of
New Jersey Institute of Technology and
Rutgers, The State University of New Jersey-Newark
in Partial Fulfillment of the Requirements for the Degree of
Doctor of Philosophy in Environmental Science

Department of Chemistry and Environmental Science

May 2011

.

APPROVAL PAGE

ENHANCED MEMBRANE DISTILLATION:
ANALYTICAL AND DEIONIZATION APPLICATIONS

Ken Gethard

Dr. Somenath Mitra, Dissertation Advisor — Date
Professor of Chemistry and Environmental Science, NJIT

Dr. Tamara Gund, Committee Member — Date
Professor of Chemistry and Environmental Science, NJIT

Dr. Edgardo. T. Farinas, Committee Member — Date
Associate Professor of Chemistry and Environmental Science, NJIT

Dr. Haidong Huang, Committee Member — Date
Assistant Professor of Chemistry and Environmental Science, NJIT

Dr. Pradyot Patnaik, Committee Member — Date
Laboratory Director, Interstate Environment Commission, New York

BIOGRAPHICAL SKETCH

Author: Ken Gethard

Degree: Doctor of Philosophy

Date: May 2011

Undergraduate and Graduate Education:

- Doctor of Philosophy in Environmental Science,
  New Jersey Institute of Technology, Newark, NJ, 2011

- Master of Arts in Environmental Management,
  Montclair State University, Montclair, NJ, 1996

- Masters of Business Administration-Finance,
  Montclair State College, Montclair, NJ, 1988

- Bachelor of Arts-Biology,
  Montclair State College, Montclair, NJ, 1975

Major: Environmental Science

Peer Reviewed Publications:

Ken Gethard and Somenath Mitra,"Membrane distillation as an on-line concentration technique: Application to the determination of pharmaceutical residues in natural waters" Journal of Analytical and Bioanalytical Chemistry, pp. 571-575, 400, March 2011.

Ken Gethard, Ornthida Sae-Khow, Somenath Mitra, "Water desalination using carbon nanotube enhanced membrane distillation" ACS Applied Materials and Interfaces, pp. 110-114, 3, February 2011.

Ken Gethard, Ornthida Sae-Khow and Somenath Mitra, "Carbon nanotube enhanced membrane distillation for the on-line preconcentration of pharmaceuticals from an aqueous phase", In review

Ken Gethard, Ornthida Sae-Khow, Madhuleena Bahdra and Somenath Mitra, "Concentration of trace inorganics in aqueous streams using carbon nanotube enhanced membrane distillation" In progress.

Ken Gethard and Somenath Mitra, "Carbon nanotube enhanced membrane distillation for on-line concentration of trace pharmaceuticals in polar solvents" Analyst, April 2011.

Ken Gethard, Phillip Sumner, et al. International Society of Pharmaceutical Engineers Best Practice Guide "Ozone Sanitization of Pharmaceutical Water Systems" April 2011.

Conference Presentations:

Ken Gethard and Somenath Mitra, "Desalination by carbon nanotube enhanced membrane distillation," Dana Know Research Showcase, NJIT, Newark, NJ, April 2010, Silver Medal Winner

Ken Gethard and Somenath Mitra, "Desalination by carbon nanotube enhanced membrane distillation," ACS Annual Meeting, Anaheim, CA, March 2011

To Sal- you are everything to me

To Gregg and Chris- you both amaze me with everything you do

ACKNOWLEDGMENT

I am indebted to Dr. Somenath Mitra, my dissertation advisor, for his constant support and guidance and for the valuable discussions and suggestions he made. I am grateful to Drs. Gund, Farinas, Huang and Patnaik for serving on my dissertation committee and for all their help.

Thanks to Gayle Katz of the Department of Chemistry and Environmental Science for all her help.

I want to thank Dr. Ed Bishop and Dr. Kamilah Hylton for all their help in getting me started with my research. Thanks to Madhuleena Bahdra and Xiangxin Meng. A very special thanks and appreciation goes to Dr. Ornthida Sae-Khow for all her support, assistance and collaboration.

Thanks to Sam Vetrano for his help with water, Don Parriott for all his suggestions with HPLC and John Lobosco for his CAD drawings. A special thanks to Brian Lee for his help with just about everything.

I also want to thank Membrana for their kind donation of the Celgard X-50 membrane material.

I am grateful to my wife, Sal, for her love and support during this adventure and to my sons Gregg and Chris for their support.

TABLE OF CONTENTS

TABLE OF CONTENTS
(Continued)

TABLE OF CONTENTS
(Continued)

Chapter **Page**

LIST OF TABLES

LIST OF FIGURES

LIST OF FIGURES
(Continued)

Figure **Page**

LIST OF FIGURES
(Continued)

Figure **Page**

LIST OF SYMBOLS

©	Copyright
EF	Enrichment factor
kl	Mass transfer coefficient- liquid boundary layer
km	Mass transfer coefficient-membrane
kp	Mass transfer coefficient- permeate boundary layer
MD	Membrane distillation
RO	Reverse osmosis
SR	Solvent reduction

LIST OF DEFINITIONS

Analyte	Compound in a matrix to be analyzed.
Concentrate	Remaining solvent that has not passed through a membrane pore and contains all the solvent impurities.
Deionization	Process to remove ionic impurities from a solvent.
Desalination	Process to remove salt from brackish or seawater.
Ion exchange	A chemical process by which ions are removed from solution and exchanged for an ion on a polymer.
Permeate	Purified solvent that has passed across a membrane pore.
Reverse osmosis	A pressurized process by which water moves across a semi-permeable membrane from an area of high salinity to an area of lower salinity.
Permeate	Purified solvent that has passed across a membrane pore.

CHAPTER 1

INTRODUCTION

1.1 Membrane Extraction

The use of membrane technology to remove or concentrate materials has developed rapidly over the past several decades. Commercial applications where membranes are commonly used include reverse osmosis for the deionization of water, ultrafiltration for the concentration of proteins in biotechnology and dialysis for the purification of blood. In all membrane extraction (ME) techniques, the membrane serves as a barrier between two phases and the membrane also controls the rate of transfer between these.[1] This action allows the enrichment of materials of interest, or conversely in a purification process it provides a means to remove unwanted materials. In ME, molecules move through membranes by the process of diffusion. Depending on the membrane type and process, movement across the membrane is driven by gradients on either side of the membrane. These include concentration (ΔC), pressure (ΔP) or electrical potential (ΔE) gradients. The process is demonstrated in Figure 1.

Diffusion across a membrane can be described by Fick's law where:

$$J = -D\, dc/dx \qquad (1.1)$$

where J is the rate of flux, D is the diffusion coefficient and dc/dx is the concentration gradient. However there are membrane factors that affect the rate of diffusion such as thickness and concentration. Their effect can be described by:

$$J = D(c_{is} - c_{il})/L \quad (1.2)$$

where c_{is} is the concentration of i at outer membrane surface, c_{il} is the concentration of i in the membrane lumen and L is the thickness of the membrane wall.

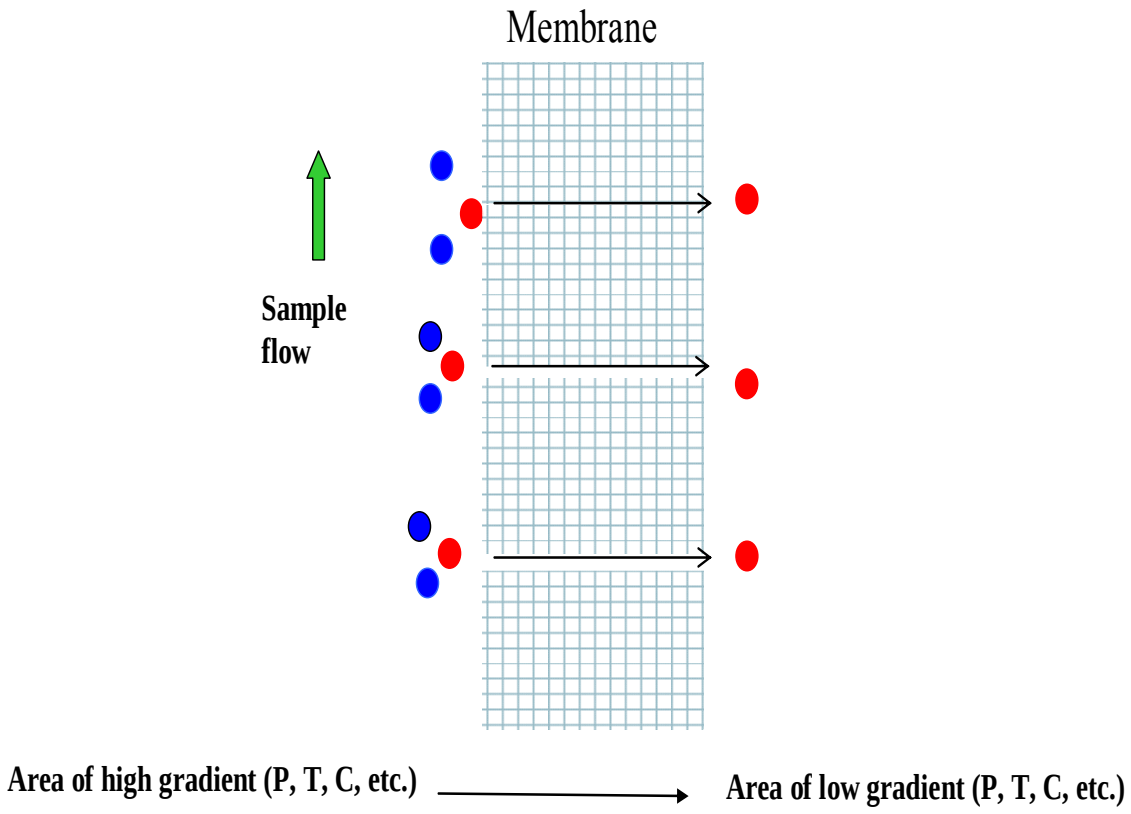

Figure 1.1 Schematic representation of permeation across a membrane. Pressure, temperature or concentration are examples of gradients that provide the driving force.

Flux can be increased by the reducing membrane thickness and ensuring there is a high gradient potential on either side of the membrane. A membrane's diffusion

coefficient is also affected by temperature, for liquids, this can be described by the Stokes-Einstein equation:

$$D= kT/n\pi a\eta \quad (1.3)$$

where k is Boltzmann's constant, a is the radius of solute and η is the solution viscosity. D increases as temperature rises resulting in a higher flux. Another factor to consider is the partition coefficient, K, where:

$$K= c_m/c_w \quad (1.4)$$

Here c_m is the analyte concentration in the membrane and c_w is the analyte concentration in feed solution. It is important to note that K decreases with temperature, while D increases under the same conditions. Therefore, increasing temperature does not always result in increased flux rate. An optimum temperature must be determined where the flux is greatest.

1.2 Analytical Membrane Extraction

Recently, membranes have been investigated as a sample preparation technique in analytical chemistry applications. The membrane can perform several sample preparation functions such as sample cleanup, extraction and concentration.[2] The interest in membranes is in large part due to their ability to enable extraction without the mixing

of two phases which in turn eliminates problems including emulsion formation and high solvent usage.[3]

The two primary membrane approaches in analytical separations are Supported Liquid Membrane Extraction (SLME) and Liquid-Liquid Membrane Extraction (LLME). These two techniques are used for analysis of a variety of materials including SVOCs, ionic compounds and metals.

The enrichment factor (EF) and extraction efficiency (EE) are two of the parameters that can be used to evaluate the effectiveness of an extraction. EF is defined as the ratio of analyte concentration in the extract to that in the initial donor:

$$EF = C_a/C_d \tag{1.5}$$

where C_a and C_d represent the analyte concentration in the acceptor after extraction and in the initial donor. EE refers to the fraction of analyte that is extracted into the acceptor:

$$EE = \frac{m_a}{m_d} = \frac{C_a}{C_d} x \frac{V_a}{V_d} = EF \frac{V_a}{V_d} \tag{1.6}$$

where m_a and m_d represent the total mass of the analyte in the acceptor and donor respectively and V_d and V_a are the volumes of the donor and extract.

In LLME, the analyte is extracted from an aqueous solution into an organic phase, so this is considered a two-phase organic-aqueous system. This technique is analogous to traditional liquid-liquid extraction but here the phases are separated by a membrane, and

are only in contact at the membrane pores. The overall efficiency of an LLME system will largely be dependent on the partition coefficient, K_p:

$$K_p = C_o/C_w \quad (1.7)$$

where C_o and C_w represent the equilibrium analyte concentration in the organic and aqueous phases respectively.

With LLME, the extractant should have low solubility in the aqueous phase and also have low volatility. The enrichment factor for polar organic compounds is typically higher than for non-polar and charged compounds. This is due to the fact the solubility of these types of compounds tends to be higher in the aqueous phase. With this application, the enrichment is driven by the concentration gradient of the analyte but is limited by the partition coefficient. This means that where the acceptor is stagnant, the more highly hydrophobic analytes will have increased efficiency because of the driving force to reach equilibrium. Therefore, enrichment and EE increase as the acceptor mobility increases.

When a liquid is immobilized in the pores of a porous material, via capillary action, the liquid can serve as a membrane, while the membrane itself functions only as a support. [4, 5] This is referred to as supported liquid membrane extraction (SLME) and can be prepared simply by immersing a porous membrane in the supporting solvent. To enhance the selectivity of the liquid membrane, a carrier molecule with a high affinity for the analyte is used. SLME is suitable for polar and ionic compounds such as organic acids, bases and metals. SLME is a three phase system where there is an organic phase between two aqueous phases. For example, in the analysis of acids, the pH of the donor

solution must be such that the compounds are in their neutral or uncharged forms, this allows them to enter the membrane. The pH of the acceptor is maintained such that once in the membrane, the analytes are extracted into the acceptor in a charged form and cannot be back-extracted into the donor. The pH gradient provides the driving force and this technique usually results in high enrichment factors. SLME offers distinct advantages such as high selectivity, donor/acceptor ratio and extraction efficiency when compared to LLME.

1.3 On-line Concentration

For trace analysis, once the analytes have been extracted into a solvent, a concentration step is generally necessary. While there has been much attention placed on on-line extraction techniques, a significant development in on-line concentration procedures has not yet occurred. With the push to develop totally automated systems, concentration procedures will need to be integrated.

Conventional analysis involves several steps: sampling at the site, transport to a laboratory, sample preparation and then analysis. The whole process takes place in separate steps at different times and places. The analysis is not on-site or on-line and takes a significant amount of time. Meanwhile, analytes are subject to evaporation, degradation, cross-contamination, etc. which can introduce errors into the analytical results. All these steps all require manual labor. The high costs of these techniques limit the number of samples that can be evaluated. Further, the delay between sampling and completed analysis compromises the capacity of immediate response in case of an emergency.

Sample preparation is a key step in the overall analytical process. The gap between sampling and analysis is partly due to the need for sample preparation. In many applications, the analyte concentration can be very low. The function of sample preparation is to convert the analytes into a high enough concentration so analysis can be completed. It is often necessary to increase the analyte concentration in order to lower the method detection limit. This is known as concentration or enrichment. It is also desirable that sample enrichment be directly coupled with an instrument so the analysis can be automated on-line and in real-time.

Current analytical concentration methods include techniques such as liquid-liquid solvent extraction (LLE), co-extraction, coprecipitation, electrolytic, sorption, gas purging and evaporative techniques such as Kuderna-Danish evaporative concentrators. All are widely used, but there are disadvantages with them. First, they are relatively complex requiring multiple steps, use of elutants or specialized equipment, and personnel using these require a significant level of training and expertise. Second, all the concentration techniques require sampling, transportation and then sample preparation in a laboratory. They are not capable of real-time applications so their utility is limited in that analytical results are from past events, they can not be used for online monitoring and control.

In contrast, an on-line membrane concentration technique could be used to sample a process stream allowing concentration in real-time and subsequent feed of the treated sample to in-line analytical instruments (e.g., HPLC, UV-VIS, MS, etc.). On-line concentration of a sample would also eliminate variables such as operator error, contamination, evaporation and degradation of labile samples. In general, on-line

methods reduce sample handling and hence the probability of analytical errors and sample loss.

Membrane separation has been interfaced with mass spectrometers in a technique referred to as membrane introduction mass spectrometry (MIMS). In this configuration the sample is constantly introduced to the membrane and the permeate is pulled by vacuum into the ion source. Various membrane media has been investigated for use in environmental analyses [6-8] for semi-volatile compounds. Membranes have also been used in the food industry for real-time monitoring of bio-reductions by bakers yeast [9], and for concentrating o-nitrotoluene and methyl salicylate in air.[10]

Another on-line version of membrane concentration is gas injection membrane extraction (GIME). This involves the introduction of an aqueous sample by a N_2 stream which injects the sample into the membrane. The membrane serves as a selective barrier through which organic analytes permeate. On the permeate side, a counter-current gas stream strips the organics and transports them to a microtrap. The retained VOCs are desorbed from the microtrap by an electrically generated temperature pulse. Rapid heating generates a concentration pulse which serves as an injection for chromatographic separation.[11] Continuous monitoring is achieved by making a series of pulses (or injections) and a chromatogram corresponding to each pulse is obtained.[12,13] The advantage of gas injection is the gas cleans the membrane and destroys the boundary layer on its surface. This method is also simpler in terms of instrumentation and operational procedures.[14]

SVOCs refer to compounds that are not readily volatilized and include compounds such as PAHs, PCBs, biomolecules, acids, phenols and pesticides. Both

SLME and LLME techniques can be applied to these compounds.[15-26] Methods that have been successfully developed integrating these techniques include online analysis of nonpolar and polar SVOCs, and automated HF-protected dynamic liquid phase microextraction (LPME).

On-line LLME is basically an automated liquid-liquid extraction across a membrane, which allows faster sample throughput, less sample handling and continuous monitoring of non-polar analytes. Online LLME has been demonstrated to effectively monitor the concentration of different SVOCs in water with the time between injections limited by the separation time.

With on-line LLME, the extractant may be static or flowing.[27] Automated On-line LLME has been reported for PCB determination[28] , herbicides in milk [29], and anesthetics in blood [30] among other applications.[31-33] On-line LLME could be further improved by simultaneous concentration. It has been[34] demonstrated that further enrichment was possible by selectively eliminating some of the extractant. It was found that solvent loss was maximum for water soluble solvents such as methanol, acetonitrile and isopropyl alcohol. The enrichment factor was directly related to solvent loss. This was an effective, yet simple technique for combining extraction and concentration in the same step.

1.4 Pervaporation

Pervaporation is an alternative to processes such as distillation and evaporation due to its low energy requirements. Pervaporation is a clean technology, particularly when used for the treatment of volatile organic compounds. With pervaporation, the separation is not

based on relative volatilities (as with thermal processes), but rather is based on the relative rates of permeation through a membrane. Pervaporation then is a combination of evaporation and gas diffusion in a single module.[35] A typical pervaporation system consists of a suitable membrane in a module, a delivery system for liquid feed, and a vacuum or a sweeping gas on the permeate side. This type of apparatus has been used in a wide range application including the analysis of various organic pollutants [36-39] and inorganic compounds,[40-43] and has been directly interfaced with gas chromatography (GC), spectrophotometry, capillary electrophoresis (CE), liquid chromatography (LC) and mass spectrometry (MS).[44-47] In the pharmaceutical arena, this technique has been reported as being used in the preparation of a variety of materials such as tablets and toothpaste.[48-50] Pervaporation has also been reported to have been used in a variety of food preparation analysis, including liquid, slurries, and solid matrices. [51-55]

Pervaporation involves both permeation and evaporation, and it is based on the selective separation of a feed liquid. Removal of the analytes from the sample is accomplished by a partial pressure differential created on the feed and permeate sides of the membrane. Separation in pervaporation is a function of the rate of permeation of a solvent across the membrane. The sample flows on one side, while the vacuum or sweeping gas is applied on the other side. The process is demonstrated in Figure 1.2. With this technique, both the feed and permeate solutions can flow continuously which leads potentially to the development of real-time monitoring techniques.

Solution-diffusion is generally the accepted mechanism in pervaporation for mass transport through non-porous membranes.[56] The permeation through the membrane consists of the following steps:[57]

(1) Diffusion through the liquid boundary-layer on the membrane feed side.

(2) Selective partitioning of molecules into the membrane.

(3) Diffusion across the membrane under a concentration gradient.

(4) Desorption into the vapor phase on the permeate side.

(5) Diffusion away from the membrane on the permeate side.

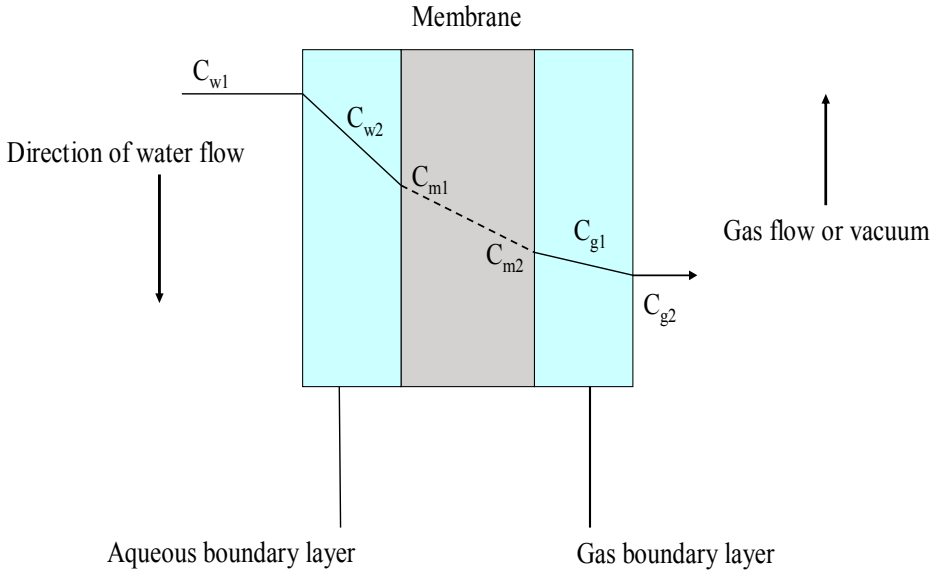

Figure 1.2 Concentration profile in a pervaporation process, where Cw, Cm and Cg refer respectively to the analyte concentration in the aqueous, membrane and gas phases.

These processes are the governing factors that control the mass transport across a membrane in a pervaporation process. The separation is due to the differences in the partitioning coefficient, diffusitivity, and vaporization of the donor components. Flux through a pervaporation membrane is determined in terms of the partial pressure difference across the two sides of the membrane:

$$J_a = P_a^G \frac{P_{ao} - P_{al}}{L} \tag{1.8}$$

where J_a is the flux for component a, L is the membrane thickness, P_a^G is the gas separation permeability coefficient, P_{ao} is the partial pressure on the donor side, and P_{al} is the partial vapor pressure in acceptor for component a.

In a pervaporative process, the vapor pressure difference is maintained by either maintaining partial vacuum or using a sweep gas on the permeate side of the membrane. The other important parameter in pervaporation is the selectivity which can be represented by the separation factor (α) and the enrichment factor (β). The separation factor of a membrane for species a and b can is defined as:

$$\alpha_{ab} = \frac{(C_a / C_b)^v}{(C_a / C_b)^L} \tag{1.9}$$

The enrichment factor is used as an indication of the separation selectivity for component a:

$$\beta = \frac{(C_a)^v}{(C_a)^L} \tag{1.10}$$

where C_a and C_b are the concentration of a and b in vapor (v) and liquid (L) phase, respectively.

With pervaporation, the operational variables are critical for controlling the process.[58] A change in the feed concentration will impact the sorption at the liquid-

membrane interface and will also affect permeation characteristics. Pressure at the feed and permeate sides is also an important characteristic.

Temperature has a major influence in the pervaporation process by affecting the analyte transport process and by altering the driving force for mass transfer. An Arrhenius-type relationship has been used to describe the effect of temperature on flux as follows:[59, 60]

$$J = J_0 \exp(\frac{E_a}{RT}) \tag{1.11}$$

where J_0 is a constant, E_a is the activation energy, R is the universal gas constant, and T is the absolute temperature.

A membrane based, on-line concentration technique using pevaporation has been developed.[61,62] With this technique selective solvent permeation leads to analyte preconcentration. The dilute solution flows into a shell and tube module, and an inert gas flows on the permeate side. The membrane preferentially allows migration of the solvent across the membrane and a more concentrated solution remains in the lumen. This was shown to be applicable to both polar and non-polar membranes for analytes such as, atrazine, pentachlorophenol, naphthalene and biphenyl. The instrumentation for analysis can be automated to concentrate either multiple samples or interfaced with chromatography.

Solvents tested using this process were hexane and methanol and the choice of the membrane used depended on whether the solvent was polar or non-polar. The combination of hexane and a nonpolar composite membrane (polypropylene with a thin

layer of siloxane) provide enrichment factors close to 20 in less than 30 seconds. Equivalent concentration in a rotary evaporator would take hours. A Nafion™ membrane was used for polar solvents such as methanol and the concentration time was similar.

On-line coupling of pervaporation to HPLC was applied to the continuous monitoring of trace pharmaceuticals in a process stream. A Nafion hollow fiber membrane module was used for monitoring 2,6-dichlorophenylacetic acid (DCPA), naphthylacetonitrile(NA), 4-chloro-3-nitrobenzophenone (CNBP), 1,2-diphenylhydrazine (DPH) and 2-chloro-3,4-dihydroxyacetophenone (CDHAP) in methanol. Analysis and detection was via HPLC-UV and enrichment factors as high as 7.9 with 91% solvent reduction were observed. The advantage of this approach is that it can provide fast (30-60 seconds) preconcentration of discrete samples for off-line analysis, and can also be performed on-line for continuous monitoring.

1.5 Membrane Distillation

Membrane distillation (MD) is a thermal evaporative process that offers advantages over traditional distillation.[63] MD can be operated at a lower operating pressure and lower temperatures than the boiling point of the feed solutions, requires lower vapor space, is unlimited by fouling and high osmotic pressure, permits a very high separation factor for non-volatile solutes has the potential for producing high-purity water or for concentrating aqueous solutions and can be used with any type of low grade heat or it can be coupled with a solar energy system. This makes it attractive for the production of potable water from brackish water in arid zones.

Membrane distillation is a technique that has undergone much investigation for both water desalination and industrial concentration applications. The interest in MD is due primarily to its low energy requirements.[64] While being a true thermal evaporative process, MD only requires relatively low temperatures (50-100ºC) to be effective. In comparison to this, traditional distillation processes operate well in excess of 100ºC. Because of this lower energy requirement, MD can potentially be operated effectively using low grade heat sources that has previously been generated for other processes.[65,66] In essence, MD can operate as a "zero-cost" energy technology and it will not contribute to global warming because no additional fossil fuels are consumed in generating heat.

Traditional evaporative techniques all have much higher direct energy requirements than does MD. For example, a very simple still would require 80,000 calories of energy to heat 1 liter of water from 20 to 100ºC.[67] Since MD can use heat already generated from other sources, this energy consumption would be avoided. Mechanical water purification processes such as reverse osmosis and electrodeionization have substantial electrical power requirements which are not required by MD. Chemical water purification processes such as ion-exchange have a high chemical energy requirement (for regeneration chemicals) and produce large volumes of chemical waste. MD does not need any regenerant chemicals and so would not produce the waste associated with these.

Membrane distillation has been known for many years, but its commercial implementation has been hampered by low water fluxes and the need for low cost heat sources. With greater emphasis being placed on energy efficiency, MD coupled with waste heat or solar energy to drive the process is being reconsidered. In particular, the

use of MD to treat brine concentrates (seawater) is receiving attention for its benefits of increased water recovery and lower brine discharges. While there is great potential for MD as an environmentally friendly process, it still requires many technological improvements to make it a useful and reliable commercial process, instead of being solely an investigative technique. The primary problem with MD is that it is a relatively low yield process. To overcome this, engineering solutions such as making more porous membrane materials have been researched, which has the disadvantage of making membranes more fragile. Another possible solution is to pack more membrane material into the same size space; however this requires special machinery and handling to achieve. Further, there are physical limits to the amount of membrane material that be contained in a defined space.[68-73]

Applications of MD to date have primarily been limited to desalination of seawater [74-83] and uses with removing water from natural food solutions (sugars, fruit and vegetable juices).[84-92] With all of these, there are fairly high levels of the material to be concentrated. For example, seawater averages a total dissolved solids content of about 34,000 mg L^{-1}.[93] Sugar syrups and fruit/vegetable juices typically have starting concentrations of 2-5% (20,000 to 50,000 mg L^{-1}). With these, MD has been shown to be effective in removing water from the concentrated solution. In the case of desalination, the permeated water is the final product, while for syrups and juice solutions the concentrated feed solution is the end product.

While pervaporation has been shown to be an effective analytical preconcentration technique for organic solvents, no work has been developed to date that would allow real time on-line preconcentration in aqueous streams. There are existing

evaporative techniques that can be used for the analytical concentration of aqueous samples, examples include Kuderna-Danish (K-D) condensers and nitrogen blowing. However, these are laboratory techniques only and are not amenable for field or on-line use.

In contrast, a technique such as MD could be used to sample a process stream allowing concentration in real-time and subsequent feed of the treated sample to in-line analytical instruments (e.g. HPLC, UV-VIS, MS, etc.). MD involves the simple removal of the solvent from the sample stream, there are no other manipulations as required with the other techniques. This simplifies the sampling preparation process and eliminates potential variability due to analyst error. If a sample stream is heated to any degree, the sample aliquot has to be reduced to ambient temperature for traditional concentration techniques. Contrasting this, a heated process stream is ideal for concentration by MD because the latent heat in the sample is used to power the process, and the resulting concentrated sample is at ambient temperature.

The principle of separation in MD is based on the difference in volatility of each substance and vapor pressure is the driving force of the process. In MD, a hydrophobic porous membrane is employed as a barrier separating heated feed and cold permeate streams. As a heated solution passes through the lumen of a hydrophobic fiber membrane, it is partially transformed to water vapor.[94]

Due to the hydrophobicity of the membrane, the aqueous solutions cannot enter the pores and a liquid-vapor interface is formed in each pore end. The hydrophobic nature of the membrane prevents the passage of the liquid phase; however, the vapor passes through the pores and is condensed on the permeate side of the membrane. The

volatile component (usually water) vaporizes at the feed interface, diffuses through the membrane's pores to the permeate interface and is then condensed into the permeate stream.

In MD processes, the penetration of liquid into the membrane's pores must be avoided, as this causes the pore to lose its hydrophobic capacity. As long as the feed pressure is kept low enough, a critical threshold known as the breakthrough pressure is not reached. The LaPlace equation describes the relation between pore size and the breakthrough pressure:

$$\Delta P = -\frac{2\mathrm{O}y\cos\theta}{r} \tag{1.12}$$

where y is the interfacial tension, O is a geometric factor related to the pore structure, and Θ is the liquid solid contact angle. This angle increases with increasing polarity difference between the polymeric membrane and the liquid. For hydrophobic membranes, the contact angle is greater than 90º.

The water transport involves evaporation into the bulk solution with higher water activity, followed by vapor transport in the gas phase and then condensation in the solution with the lower water activity. The water flux is proportional to the water vapor pressure difference across the membrane controlled by the water vapor activity difference :[95]

$$J_w = k_{mp}(p_{w1} - p_{w2)} \tag{1.13}$$

where k_{mp} is the membrane mass transfer coefficient. As mass transfer proceeds a boundary layer is formed on each side of the membrane. The water activity difference between both membrane interfaces is lower than the bulk feed resulting in the reduction of the driving force. The flux in the boundary layers can be related to the mass transfer coefficients k_1 and $k_{2\ by:}$

$$J_w = k_1(a_1 - a_{m1}) = k_2(a_{m2} - a_2) \qquad 1.14$$

where a_i is the bulk water activity and a_{mi} is the water activity at the membrane interface. A schematic representation of the water activity profile for MD is shown in Figure 1.3.

MD is similar to pervaporation [96, 97] in that the driving force is determined by a vapor pressure difference on either side of the membrane, however in MD there is also a simultaneous heat transfer involved. Typically, MD is depicted as having a liquid-vapor interface forming at the entrance to the membrane's pores where the feed stream vaporizes. Inside the pores, only a gaseous phase is present and as long as a pressure gradient is maintained, the vapor will be transported. Since the bulk feed solution has a higher temperature than does the permeate, this vapor pressure difference is maintained. A depiction of the membrane distillation process is shown in Figure 1.4.

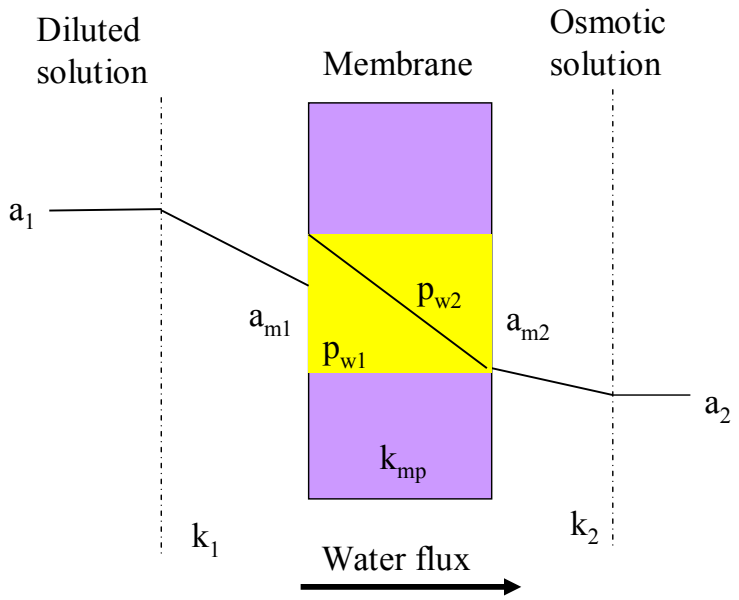

Figure 1.3 Water activity profile in membrane distillation.

While water flows on one side of the membrane, a stagnant layer is formed between it and the membrane. The overall mass transfer resistance is the sum of the mass transfer coefficients of the aqueous boundary layers on either side of the membrane, the membrane pore's resistance and the gaseous boundary layer on the permeate side. In analytical applications where thin membranes are used, mass transfer through the aqueous boundary layer is the rate limiting step.

Since MD is a thermally driven process, both heat and mass transport are involved simultaneously, and heat transfer is often the rate limiting step. There are two important mechanisms responsible for the heat transfer across the membrane. The first is conduction through the membrane material and the vapor within the membrane pore, and transfer and transfer of the heat of vaporization associated with the vapor flux.

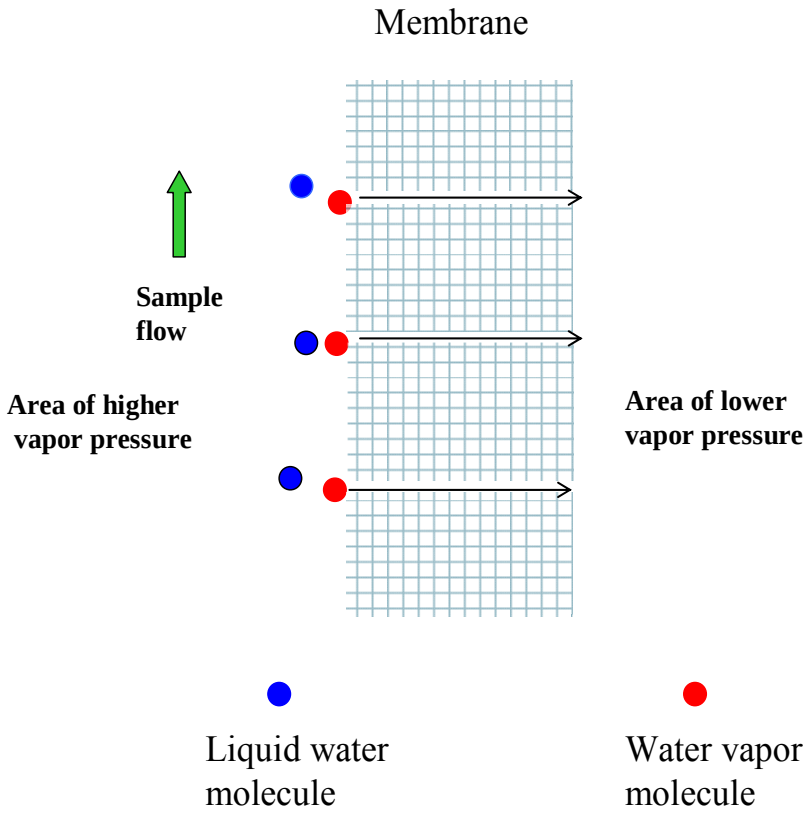

Figure 1.4 Representation of membrane distillation, vapor flows from an area of higher vapor pressure to an area of lower vapor pressure across a hydrophobic membrane.

Since there is no flux induced by the conduction of heat across the membrane, it is considered as a heat loss in the process that lowers the overall efficiency. Conductive heat loss through the membrane can rarely be controlled because of the trade off between a thick membrane for better heat insulation and a thin membrane for reduced mass flow resistance. Heat transfer can be considered in three steps. The first is convective heat transfer from the heated solution across the boundary layer to the membrane surface. The second is heat transfer across the membrane by conduction and assembling the vapor flow through the pores. The third is the convective heat transfer from the membrane

surface of the permeate side across the boundary layer to the bulk permeate solution. The heat transfer can be described by:[98]

$$Q = J\Delta H_v + \frac{k_m}{\mathrm{M}}(T_{m1} - T_{m2}) \tag{1.15}$$

where J is the flux, M is the membrane thickness, ΔH_v is the latent heat of evaporation, k_m is the thermal conductivity of the porous membrane and T_{m1} and T_{m2} at the hot and cold membrane surfaces.

However, this equation only accounts for the latent heat of evaporation. The heat transferred by conduction through the membrane is considered as heat lost so:

$$Q_{lost}^{N} = \frac{k_m}{M}(T_{m1} - T_{m2)} \tag{1.16}$$

The evaporation efficiency is defined as the ratio between the heat which contributes to evaporation and the total heat exchanged by the feed. The total heat exchanged by the feed is the difference between the sensible heat of the incoming feed stream ($Q_{1\text{-in}}$) and the sensible heat of the outgoing feed stream ($Q_{1\text{-out}}$). This total heat exchanged by the feed consists of the T_{m1} and T_{m2} and of the heat that is lost to the environment by conduction.

A large amount of heat is used to vaporize the solution, this results in a temperature difference between the bulk solution and the membrane surface, causing a temperature polarization.[99-106] This temperature polarization causes a significant loss in

the driving force of the mass transfer through the membrane. Estimates have been made that up to 30% of useful heat is lost due to this temperature polarization. This means the water vapor pressure difference calculated with the temperature at the membrane interfaces is only a fraction of the water vapor pressure difference calculated with the bulk temperature. The ratio of useful energy for the mass transfer of vapors is called the temperature polarization coefficient (TPC) and this represents the fraction of total thermal driving force that contributes to mass transfer.[107] The TPC is defined as:

$$TPC = \frac{T_{mf} - T_{mp}}{T_f - T_p} \tag{1.17}$$

where T_{mf} is the interfacial feed temperature, T_{mp} is the interfacial permeate temperature, t_f is the bulk feed temperature and T_p is bulk permeate temperature. A schematic of the temperature polarization in MD is shown in Figure 1.5

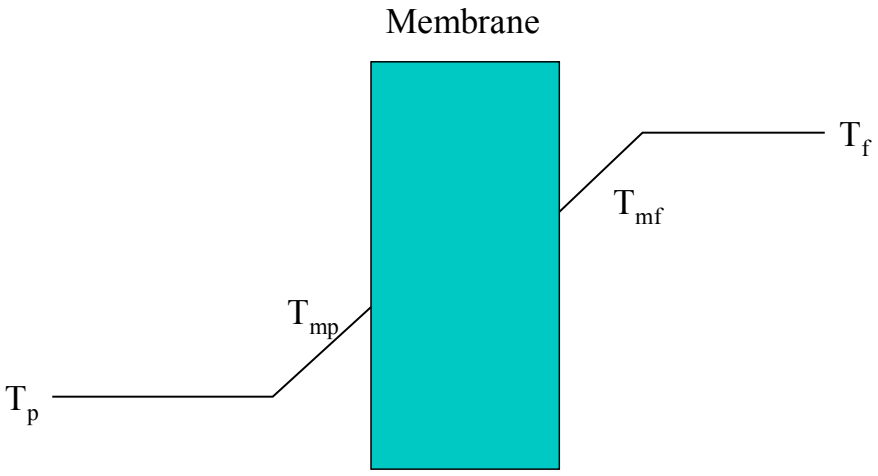

Figure 1.5 Temperature polarization in membrane distillation.

Given the evaporation and condensation rates depend on the interfacial temperatures and not the bulk temperatures, and because the vapor pressure driving force is primarily a function of temperature, it is desired the difference between T_{mf} and T_{mp} be as high as possible. In other words, a higher TPC will increase overall mass transport. It is generally thought a higher feed flow helps to overcome the temperature polarization effect. This is most likely due to increased turbulent flow that minimizes localized "hot spots" on the membrane surfaces. However, the higher pressures involved with pumping the solution faster may cause the pore's break-through pressure to be exceeded and will result in pore wetting that prevents further vapor transport.

With MD, mass transfer is separated into three steps, mass transfer in the feed boundary layer, mass transfer across the membrane and mass transfer in the permeate boundary layer. The Dusty gas model (DGM) is generally used to explain mass transfer across a membrane's pore in MD. With the DGM, the pore's medium is viewed as a grouping of uniformly distributed dust particles held stationary in space. The presence of gas-surface interactions considers the gas molecules as large particles. This model is composed of four components: molecular (Fickian) diffusion, Knudsen diffusion, surface diffusion and viscous flow [108] as shown in Figure 1.6. Molecular diffusion is used in circumstances when collisions between molecules play the main role in mass transport. The Knudsen diffusion model is followed whenever collisions between molecules and the pore's wall are the dominant transport mechanism. Surface diffusion represents flow when a solute molecule adsorbs on the surface of the pore and then hops from one site to another based on interactions between the surface and the molecules. Viscous flow is the flow of a gas across a channel under conditions where the mean free path is small in

comparison to the transverse section of the channel and the flow characteristics are determined mainly by collisions between the gas molecules.

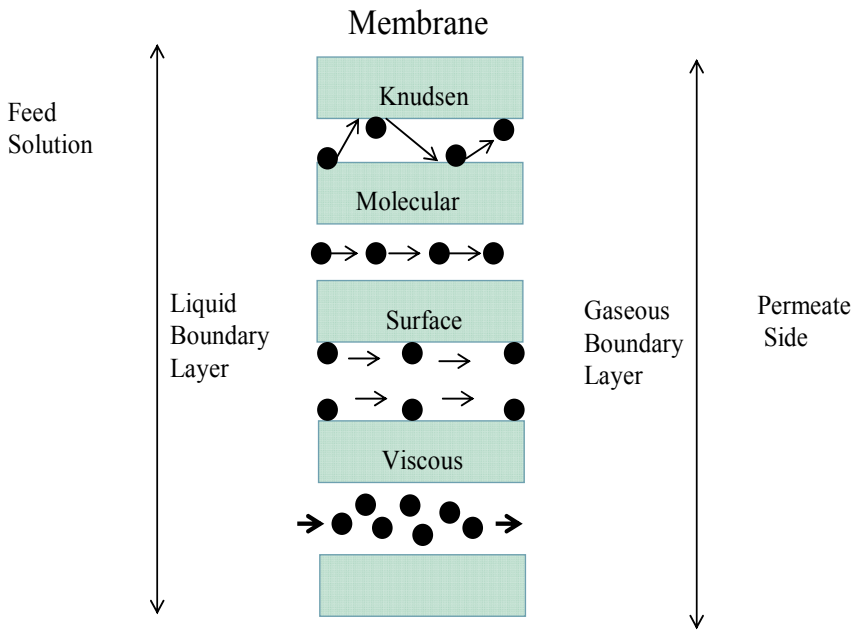

Figure 1.6 Membrane distillation diffusion mechanisms across hydrophobic membrane pores.

When considering only Knudsen or molecular diffusion, the molar water flux (N_w) can be described by:

$$N_w = -\frac{1}{RT}\left(\frac{1}{D_{we}^{k}} + \frac{p_{air}}{D_{w-air}^{oe}}\right)^{-1} v_{pw} \qquad (1.18)$$

where p_{air} is the air partial pressure, R is the gas constant, T is absolute temperature and D^{k}_{we} and $D^{oe}_{w\text{-}air}$ are the Knudsen and molecular diffusivities.

Usually in MD, mass transport is typically explained in terms of only Knudsen or molecular diffusion.[109] As membrane pore size decreases (to less than 0.2 micron), Knudsen forces predominate, and conversely as pore diameter increases, molecular diffusion is the dominant transport mechanism. To date, surface diffusion and viscous flow have not been considered as major contributors in MD. Further, the mass transfer boundary layers at the bulk feed-membrane and permeate-membrane interfaces are thought to result in negligible contributions to overall mass transfer resistance.

In a thermally driven MD process, the increase in the overall resistance to mass transfer as a result of the presence of a mass transfer boundary layer in proximity of the membrane interface is generally ignored. However, this must be considered if crystallization or precipitation processes can occur, because these might induce supersaturation in the proximity of the membrane.

A mass balance across the feed side boundary layer allows a relationship to be derived between molar flux (J), the mass transfer coefficient (k_x) and the solute concentrations c_m and c_b at the membrane interface and in the bulk:

$$\frac{J}{p} = k_x \ln \frac{c_m}{c_b} \tag{1.19}$$

where p is the density of the solution.

A phenomena known as concentration polarization occurs when solvent permeates through the membrane, and the solute concentration c_m at the feed solution/membrane interface becomes higher than in the bulk solution, c_b. This is quantified by:

$$CPC = \frac{C_m}{C_b} \tag{1.20}$$

where CPC is the concentration polarization coefficient. While there is known concentration polarization in reverse osmosis, it generally is not considered as a significant concern with MD.

Membranes that are most suitable for MD processes should have the following properties:

- Small thickness and low tortuosity
- Low thermal conductivity of the membrane material
- High porosity to lower conductive heat flux and increase water vapor transport
- Reasonable pore size, but balanced by preventing membrane pore wetting
- Low surface energy or high hydrophobicity so the membrane is applicable under high pressure.

1.6 Objectives

The objective of this research was to develop analytical preconcentration techniques using membrane distillation as the evaporative process. Further, carbon nanotubes were immobilized into the membrane's pores (CNIM) and comparative studies were completed to determine if this improved the overall efficiency of the MD process. Based on favorable results obtained with CNIM in analytical applications, further work was completed on water desalination and deionization applications using CNIM. This work is presented in five parts.

Part 1 Membrane Distillation as an On-line Concentration Technique

Membrane distillation (MD) was investigated as a real-time, online concentration technique, where the aqueous matrix is selectively removed from the sample to enhance analyte enrichment. This technique was aimed at exploring the possibility of using MD as a universal method for a wide range of compounds and is unlike conventional membrane extractions that rely on the permeation of the solute into an extractant phase

Part 2 Carbon Nanotube Enhanced Membrane Distillation for On-line Preconcentration

Carbon nanotube enhanced membrane distillation was investigated as a means to preconcentrate pharmaceutical residuals in water. It was demonstrated that CNT immobilized membranes enhanced the level of preconcentration as compared to standard membranes.

Part 3 On-line preconcentration of trace pharmaceuticals in polar solvents using carbon nanotube enhanced membrane distillation

Carbon nanotube enhanced membrane distillation was investigated as an on-line analytical preconcentration technique to provide real time monitoring of impurities in pharmaceutical processes where methanol is recovered. In a carbon nanotube immobilized membrane (CNIM), the carbon nanotubes (CNTs) provide additional pathways for solvent vapor transport.

Part 4 Water Desalination Using Carbon Nanotube Enhanced Membrane Distillation

Desalination is the process by which high levels of salts are removed from water allowing it to be used as drinking water. Carbon nanotube enhanced membrane distillation was investigated as a means to improve desalination efficiency as compared to traditional membrane distillation.

Part 5 Concentration of trace inorganics in aqueous streams using carbon nanotube enhanced membrane distillation

With this work dilute aqueous solutions of various inorganic compounds were concentrated using carbon nanotube enhanced membrane distillation. The carbon nanotubes (CNTs) served as a means to increase vapor transport capacity resulting in greater water loss.

CHAPTER 2

MEMBRANE DISTILLATION AS AN ON –LINE CONCENTRATION TECHNIQUE: APPLICATION TO THE DETERMINATION OF PHARMACEUTICAL RESIDUES IN NATURAL WATERS

2.1 INTRODUCTION

The objective of this work [110] was to explore MD as an on-line and real-time concentration technique for analytical applications. Of particular interest is the monitoring of semivolatile organics such as drug molecules in aqueous matrices. In recent days these compounds have become public health concerns, and have been classified as emerging contaminants.[111-113]

Another example of where MD may have an analytical application is with pharmaceutical equipment cleaning. In pharmaceutical manufacture, it is very important to ensure that all traces of pharmaceutical ingredients are removed from equipment prior to using that equipment for another product.[114] Equipment is cleaned and then repeatedly rinsed with either hot Purified Water or with an organic solvent. The process of ensuring equipment is adequately cleaned is referred to as cleaning verification. Cleaning verification involves taking "grab samples" of rinsate and then analyzing these off-line in a laboratory. This process is time consuming, expensive and generates large volumes of waste solvent.

In 2002, FDA recognized this problem and launched their risk-based approach initiative [115] in order to encourage the use of the latest advances in pharmaceutical technology. One aspect of this initiative is to use Process Analytical Technology (PAT). PAT is a system for analyzing and controlling manufacturing through continuous

measurements of critical process attributes. Most PAT initiatives to date have focused on batch processing of tablet products using techniques such as NIR, Raman, acoustics and particle monitoring. PAT has not been studied to date for pharmaceutical equipment cleaning. Its application to this area would provide both environmental benefit (from reducing the amount of solvents and energy used) as well as an economic benefit.

With the PAT concept, verification of equipment cleaning would be completed at-line using the same analytical techniques as used for analysis of the active ingredient in the drug product. The referee method to quantify active ingredients usually is HPLC; however the limit of detection is often not low enough to detect the levels found in rinse samples. Using MD as an in-line concentration technique would take advantage of the residual heat from the heated rinse solvents and the cooled, concentrated sample could be fed directly to an HPLC column. This real-time analysis would allow for reduced cleaning time and reduced rinse requirements.

2.2 Experimental

Celgard type X-50 hollow fiber membrane (courtesy of the Membrana-Charlotte division of Celgard, LLC, Charlotte, North Carolina, USA) was used for all experiments. This material has been used extensively in water degassing operations.[116,117] Physical dimensions of the X-50 membrane are: wall thickness 80 microns, inner diameter 220 microns, porosity, 40%. Nominal pore size for this membrane is 0.04 micron, so Knudsen diffusion would be expected to be the primary diffusion mechanism.

Membrane modules were constructed in a shell and tube format using threaded brass pipe fittings**.** The "shell" portion of the module was a ¼ inch ID X 1.0 inch long

pipe nipple. To each end of this was attached a T fitting, through which the membrane was introduced. A total of 36 membrane strands were used in each module, total membrane contact surface area (based on internal membrane ID) was 0.84 cm^2. The ends were then sealed with epoxy to prevent leakage into the shell side and the assembled module was insulated with fiberglass insulation. Component parts and an assembled module are shown in Figure 2.1

One of the vertical legs of a T-fitting was attached to a vacuum source using polyflo tubing. When vacuum was applied, room air came in through the other drain port and exited through the second drain port. Vacuum was regulated so that air volume through the membrane module was 1 L min^{-1}. A space heater was used to heat the air entering the module.

Test solution was pumped through the module using a Hewlett Packard (Palo Alto, CA., USA) HPLC 1050 pump. The solution traveled through 1/8 inch teflon tubing that was coiled and immersed in a water bath at a set temperature. The teflon tubing was connected to the inlet of the module. As solution traveled up the length of the module, permeate was discharged through the drain port fitting.

Four pharmaceutical active ingredients were studied: ibuprofen (an anti-inflammatory) dibucaine (a topical anesthetic), acetaminophen (an analgesic) and diphenhydramine (an anti-histamine). All reagents and chemicals used in this work were purchased from Sigma-Aldrich (Saint Louis, MO, USA). A schematic of the membrane module and experimental set up is shown in Figure 2.2.

2.1a

2.1b

Figures 2.1 (a) Component parts of the membrane module (b) assembled module.

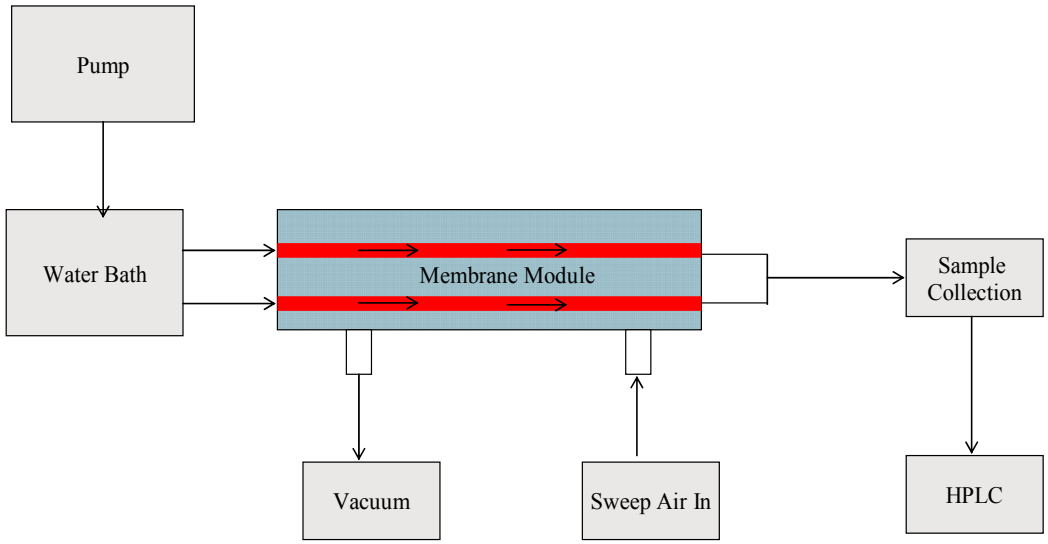

Figure 2.2 Schematic diagram of the experimental system.

All analysis was completed using a Hewlett Packard HPLC system and a Perkin Elmer (Waltham, Ma, USA) 785 UV-Vis analyzer. The diphenhydramine was determined using a Zorbax SB-CN 250mm x 4.8 mm column. Ibuprofen, acetaminophen and dibucaine were determined using Supelco C-18 250 mm x 4.6mm columns. SRI's (Torrance, CA, USA) Peak Simple Version 3.29 was used for HPLC data analysis. Analysis for ibuprofen, dibucaine and diphenhydramine were carried out using procedures detailed in the USP.[118] The analysis for acetaminophen was completed using a method found in the literature.[119] A 5 mg L^{-1} ibuprofen solution was used for all process optimization experiments.

2.3 Results and Discussion

For analytical enrichment, the two important factors are the preconcentration of analyte and the reduction of the amount of solvent. The enrichment factor (EF) is directly related to the analytical sensitivity, and the solvent reduction (SR) determines the amount of solvent removed in MD. A higher SR leads to higher EF.

An important consideration is the effect of membrane surface area. The membrane flux as a function of surface area can be calculated by:[120]

$$J = \frac{w^p}{tA} \tag{2.1}$$

where J is the flux, w^p is the total mass of permeate collected, t is the permeate collection time and A is the membrane surface area.

Three modules were prepared with 6, 12 and 36 hollow fiber membrane strands, and represented 0.14, 0.28 and 0.84 cm^2 of membrane surface area (based on internal

diameter). Experimental results using a 5 mg L^{-1} ibuprofen solution at 90ºC and 0.5 ml min^{-1} are summarized in Figure 2.3. Data showed a strong correlation between membrane surface area and both EF and SR. The response was nearly linear with membrane surface area.

It is worth mentioning that MD is also a thermal process, where temperature gradients play important roles. For example, in an adiabatic measurement, a sample at 80ºC was found to exit the membrane module at 20-25º because much of the thermal energy is lost as latent heat in MD. Therefore, membrane configuration is expected to play an important role. In addition to the above experiments with modules of different surface area, a fourth membrane module was prepared where the total membrane surface area was the same as for the 36 strand module (0.84 cm^2) but was twice as long because it used only 18 strands. EF and SR for this were approximately 30% lower than for the 36 strand module. This indicated that vapor flux decreased as the aqueous solution moved down the module, which was attributed to evaporative cooling that took place when the vapor was removed. Therefore, a high surface area membrane module with short residence time is a recommended design for MD.

The effect of feed flow rate at constant temperature (90ºC) is shown in Figure 2.4. At lower flow rates the residence time was higher and there was more time for vapor permeation. The overall effect was that EF and SR decreased with increases in flow rate.

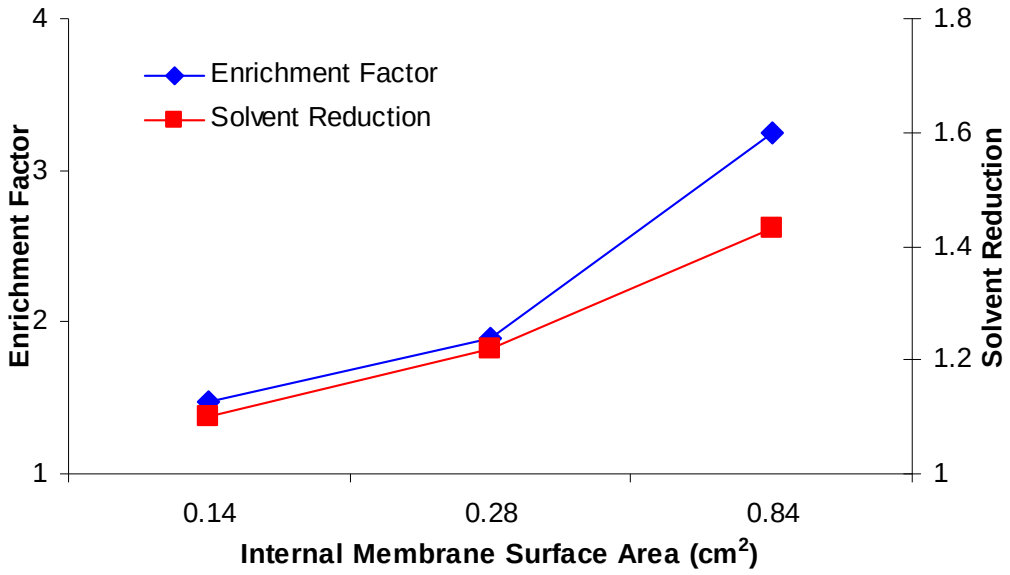

Figure 2.3 Effect of membrane surface area on EF and SR.

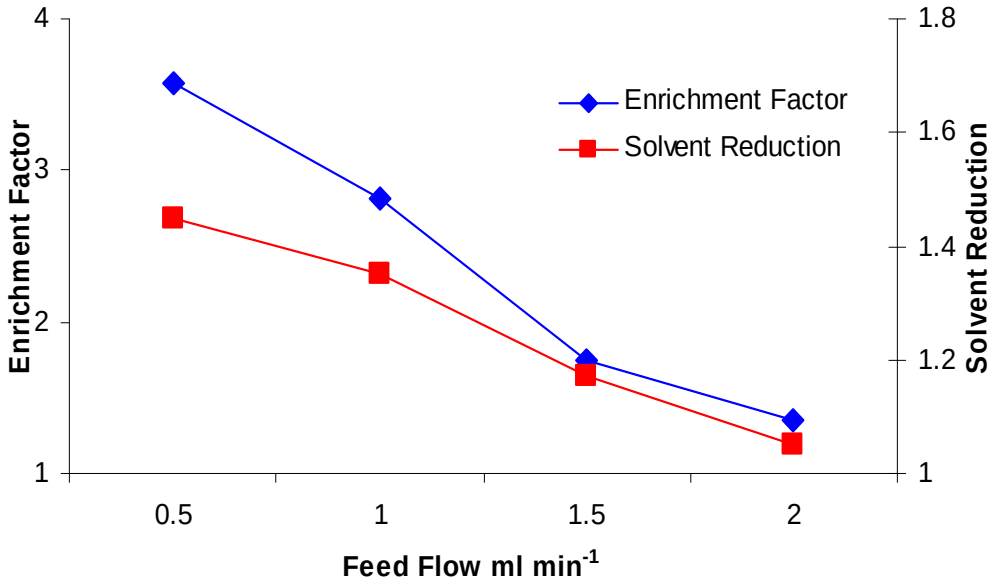

Figure 2.4 Effect of feed solution flow rate on EF and SR.

Temperature is an important factor that affects both vapor pressure and diffusion coefficient. Higher temperatures lead to higher vapor pressure, which increase exponentially with temperature [121] and the diffusion coefficient followed an Arrhenius type temperature function. Experimental results for varying temperatures under constant flow and feed solution concentration are shown in Figure 2.5. The data showed an increasing feed solution temperature enhancing both SR and EF. The data show a maximum in the curves. Both SR and EF peaked around 90ºC and then dropped as the temperature was raised to 100°C. A possible explanation for this is that at higher temperatures, the vapor may not be "dry" and carry small water droplets with it. The presence of liquid would tend to occlude membrane pores which would decrease overall permeability.

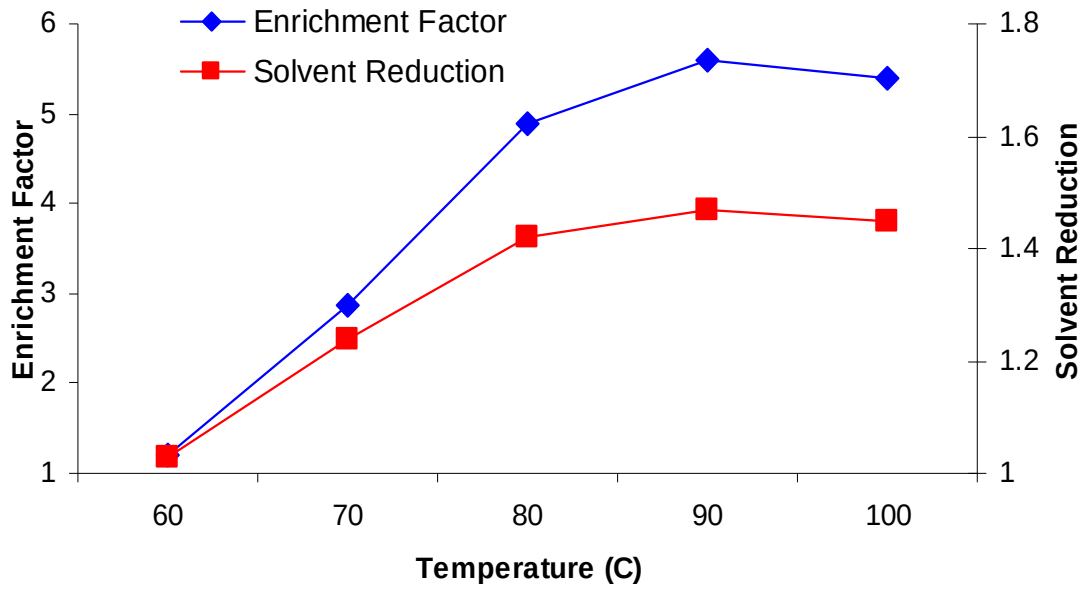

Figure 2.5 Effect of feed solution temperature on EF and SR.

2.4 Analytical Performance

In addition to ibuprofen acetaminophen, diphenhydramine and dibucaine were also studied. All four compounds were tested at constant flow of 0.5 ml min^{-1}, 90ºC and using the 36 strand membrane module. All measurements were repeated in triplicate. EF for the individual compounds varied between 3.6 and 5.6. Further, all four compounds were also tested in triplicate by thermal evaporation at 90°C and 30 minute heating.[122, 123] Data comparing the two procedures is summarized in Table 2.1.

MD was highly reproducible with RSD ranging between 3% and 5% and accuracy as relative percent error was less than 2%. In comparison, enrichment factors by thermal evaporation were similar, ranging from 3.0 to 4.6 but had higher RSDs (ranging from 4-9%). With MD, compounds showed linear calibration in the range of 0.05 to 20 mg L^{-1} with an r^2 greater than 0.994. This made quantification using external standards feasible. The method detection limits at a signal to noise ratio of three were 0.01 mg L^{-1}, 0.03 mg L^{-1}, 0.05 mg L^{-1} and 0.03 mg L^{-1} for ibuprofen, acetaminophen, diphenhydramine and dibucaine respectively. Lower detection limits could be achieved by increasing the number of hollow fibers, thus increasing useful surface area.

These studies demonstrate that MD is a promising approach for online and real time concentration of trace impurities in pure water samples. It should be noted that MD is a preconcentration process. It can be coupled to micro/nanofiltration and other clean up techniques to provide those functions. In general, MD offers several advantages that are uniquely suited for on-line monitoring of a wide range of semi-volatile compounds.

Table 2.1 Enrichment Factor and Solvent Reduction for Various Pharmaceutical Compounds, Comparing MD and Thermal Evaporation (1.0 mg L^{-1} feed solution at 90°C)

	EF by MD	% SR by MD	EF by Evaporation	%SR by Evaporation
Ibuprofen	5.6	48	4.6	59
Acetaminophen	3.6	35	3.0	51
Diphenhydramine	5.1	47	4.2	58
Dibucaine	3.6	40	3.0	53

Based on the results presented here, it is particularly useful to the pharmaceutical industry to monitor various process and waste streams. For example, in pharmaceutical reactor cleaning where hot Purified Water is routinely used, MD can use waste heat from cleaning solutions to concentrate the sample in real time and the evaporative cooling would allow direct interfacing to HPLC. Potentially, MD can replace the conventional grab-sample followed by laboratory analysis reference with simple on line instrumentation.

2.5 Conclusions

MD was found to be an effective real-time concentration technique where the enrichment occurred via the elimination of water from an aqueous sample. Temperature, feed flow rate, total membrane surface area and membrane configuration were all important parameters and EFs as high as 5.6 were obtained. The process was linear over the concentration range studied and the method showed excellent figures of merit along with low detection limits.

CHAPTER 3

CARBON NANOTUBE ENHANCED MEMBRANE DISTILLATION FOR ON-LINE PRECONCENTRATION OF PHARMACEUTICALS FROM AN AQUEOUS PHASE

3.1 Introduction

While MD offers the opportunity to partially removal the aqueous matrix for preconcentration, it is limited because of the relatively low enrichment. The objective of this work is to investigate the comparative enrichment capabilities of two membrane modules. The first module was the same as that used for the experiments in Chapter 2. The second membrane module was identical except that carbon nanotubes were imbedded in the membrane pores. Recently, novel membranes have been developed by immobilizing carbon nanotubes (CNTs) into membrane pores.[124] Referred to as the carbon nanotubes immobilized membrane (CNIM), here the CNTs serve as a sorbent and provide an additional pathway for solute transport.[125-127] The objective of this work was to implement CNIM as the membrane to provide enhanced preconcentration in MD. Of particular interest is the monitoring of semivolatile organics such as drug molecules in aqueous matrices from effluent streams and wastes from the pharmaceutical industry. In recent days, these compounds have become important and have been classified as emerging contaminants.

In all membrane processes, the key component is the membrane itself because it determines both flux and selectivity. The development of a novel membrane architecture is of great importance to enhance the membrane performance.

Carbon nanotubes (CNTs) can be described as a graphite sheet rolled up into a nanoscale-tube. These CNTs have diameters ranging up to tens of nanometers and

lengths up to several centimeters with both ends normally capped by fullerene-like structures.[128] CNTs have high stiffness and axial strength due to their carbon-carbon sp^2 bonding. The highly developed hydrophobic surface of CNTs exhibit strong sorption properties towards small gas molecules. This sensitivity is largely based on charges in the electrical properties of the CNTs. CNTs have also been shown to have capacity for sorption of inorganic ions in not only the outer surfaces but also in the inner cavities, and the intra-layers in the structure of a CNTs are responsible for moving the ions. The physico-chemical properties of CNTs are known to play an important role in membrane processes, where the nanotubes serve as channels for mass transport of water vapors and gases [129, 130] and the high flux has been attributed to the atomic-scale smoothness of the CNT walls as well as molecular ordering inside the nanopores.[131] Studies have shown that absorbed water molecules tend to organize themselves into a long lasting hydrogen-bonded network.[132,133] Further, pulse like burst transmissions of water molecules through the CNTs have been observed. These bursts are due to the tight hydrogen bonding network within the tube which ensures that density fluctuations lead to controlled and rapid motion through the nanotube. The water molecules are conducted through the nanotube and move with little resistance unhindered by interactions with the hydrophobic wall of the CNT. Further, the flow appears to be frictionless and is limited primarily by the barriers at the entry and exit of a nanotube pore and flow rates are independent of the length of the nanotube.

In the CNTs, water molecule entry, exit and transport are highly correlated and the tightly coupled motion of the water chain can be described as a continuous random walk. For the single-file flow of water molecules within a CNT, flow friction with the wall does not slow down the water transport. This corresponds to an almost perfect slip

boundary condition within the CNT pore. Water flow then is independent of the channel length and is limited mainly by molecule entry and exit events. The net average flow rate per tube is determined by the thermodynamic driving force and is limited by the activated diffusion hopping rate. Since CNTs act as both molecular transporters and sorbents, [134] they can increase the permeability of a substance through a membrane as well as increase its selectivity. The CNTs also increase functional surface area in the membrane system due to their high aspect ratio.[135] Furthermore, particularly pertinent to MD, is the fact that the high thermal conductivity of the CNTs may reduce the temperature gradient at membrane interfaces, allowing for reduced surface tension.[136, 137] All these mechanisms are expected to play important roles on the molecular transport of water vapors in the presence of the CNTs and lead to enhanced performance in MD.

Flow through CNTs is assumed to follow Knudsen diffusion models.[138] However, measured fluxes are high enough so that free molecular transport is indicated. Flux results one to two orders of magnitude higher than expected were measured. This observed increase in flow enhancement is most likely caused by the intrinsic smoothness of the CNT surface. In the atomically smooth walls, the nature of the gas-wall collisions can change from purely diffuse (Knudsen) to a combination of specular and diffuse collisions. Flow rates across CNTs have been measured that are several orders of magnitude than would be predicted by a no-slip hydrodynamic flow as calculated by the Hagen-Poiseulle equation. This is not unexpected since the diameters in a CNTs tube lie between slip flow and transitional flow regimes.

The presence of CNTs affect membrane characteristics such as diffusion coefficient and geometric factors (defined as porosity and shape factor, etc.) [139, 140] while the partition coefficient is affected by the excellent sorbent characteristics of the CNTs.

Figure 3.1 depicts the proposed mechanisms for the selective transport of water vapors during MD across a carbon nanotube enhanced membrane. Immobilizing the CNTs in the pores altered the water-membrane interactions, which is one of the major physicochemical factors affecting the permeability and selectivity of the membrane .

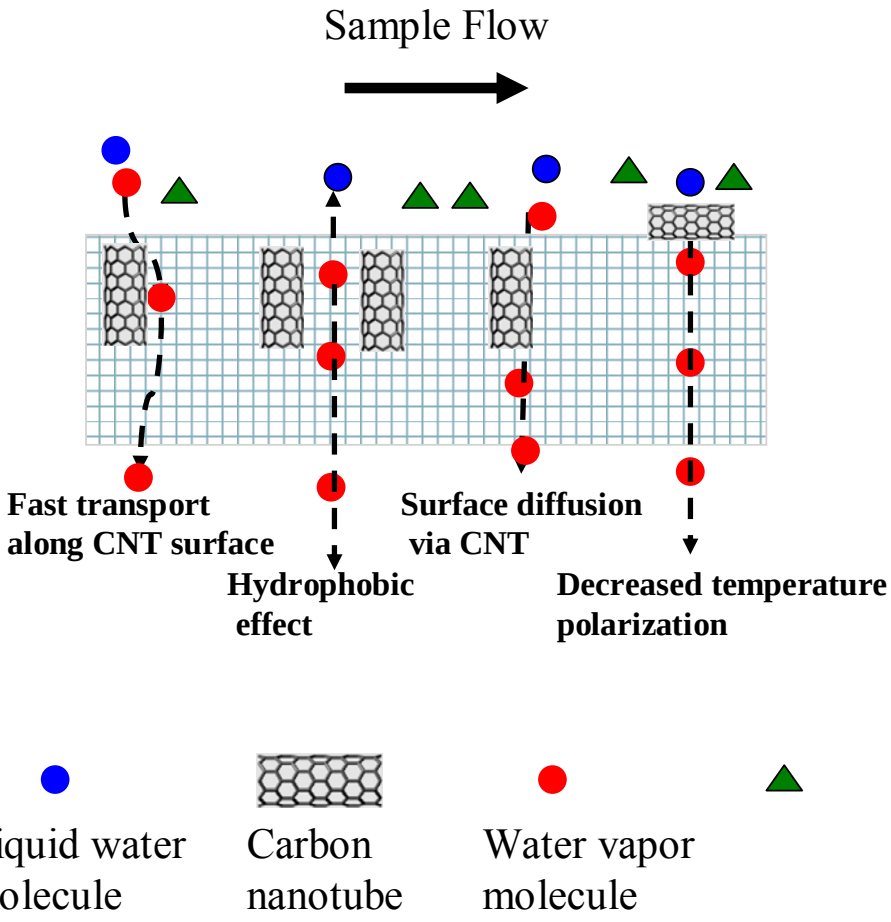

Figure 3.1 Schematic diagram of mechanisms of action of CNIM.

Since CNTs are highly hydrophobic, they decrease the tendency of a pore to become wet with liquid, so more pure vapor transport can occur. Different mass transport mechanisms are possible within CNT pores including convection, molecular diffusion, Knudsen diffusion and surface diffusion. It is generally assumed that gas flow across a membrane's pore follows Knudsen or molecular diffusion transport mechanisms. Since CNTs are known to have rapid sorption and desorption capacity, it is possible they allow the water vapor molecules to follow a surface diffusion pattern, in which the water molecules hop from one site to another by interacting with the surfaces. This action increases overall vapor transport. If there is a high enough concentration of molecules adsorbed on the wall of the CNT they may exhibit mobility. Transport by movement of molecules over a surface is partially due to the differences in molecular densities between the adsorbed and vapor phases. Surface diffusion is an activated process and it diffusivity is described by an Arrhenius function. If there is a difference in total pressure between the ends of the CNT pore, there will be bulk flow, according to a form of Poiseulle's equation. Bulk flow becomes more important as pressure and the pore diameter increase. The resultant diffusivity for a given component, incorporating the contributions from all mass transfer mechanisms can be expressed as:

$$D_{total} = \frac{1}{\frac{1}{D_k} + \frac{1}{D_m}} + D_{poiseulle} + KD_{surface} \tag{3.2}$$

where K is the dimensionless adsorption equilibrium constant.

The CNTs also provided an alternate route for fast mass transport via diffusion along their smooth surface. The water vapor may also be transported directly through the inner tubes of the CNTs, which are known to enhance vapor transport.

The condensation of water is known to reduce the hydrophobicity of the membrane leading to the attraction of more water molecules which may eventually lead to pore clogging. The presence of CNTs reduces these effects. Since CNTs are highly hydrophobic, they decrease the tendency of a pore to become wet with liquid, so higher transport of pure vapor can occur.

It is well established that CNTs have high thermal conductivity and in fact, CNTs display the highest measured thermal conductivity of any known material at moderate temperatures . The additive effect of CNTs to the thermal conductivity of a membrane can be estimated by:[141]

$$\frac{K_c}{K_m} = 1 + \frac{fK_c}{3K_m} \tag{3.3}$$

where K_c is the thermal conductivity of the liquid, K_m is the matrix phase (e.g. membrane material) thermal conductivity and *f is* the volume fraction of CNTs. This relation demonstrates the large thermal conductivity enhancement induced by the CNTs. The higher thermal conductivity of the CNTs reduces the temperature gradient in the membranes, thus reducing condensation and allowing more vapor to permeate through the pores. Further, the more equal temperature distribution across the pore's length helps to lower the surface tension [142, 143] in the pores allowing easier transport of water vapors.

Another possible effect is reduced temperature polarization.[144-147] As seen in Figures 3.2 b, 3.2d and 3.2f, CNTs lay on top of the membrane as well as in the

membrane pores. It is possible the CNTs here reduce the temperature polarization between the bulk feed and membrane interface allowing an overall more efficient process.

3.2 Experimental Section

The carbon nanotube immobilized membranes (CNIM) were prepared as follows. Ten milligrams of multi wall nanotubes (Cheap Tubes, Inc, Brattleboro, VT, USA) were dispersed in a solution containing 0.1 mg of polyvinylidene fluoride (PVDF) in 15 ml of acetone by sonicating for an hour. The PVDF/CNTs dispersion was forced under vacuum into the pore structure of the polypropylene membrane. The CNIM was produced during this step and the PVDF served as a binding agent that held the CNTs in place. The membrane was then flushed with acetone to remove excess CNTs and PVDF. Experiments were carried out using modules with CNIM as well as plain membranes without CNTs. The two modules used were the same in construction to that described in Chapter 2 (i.e. 36 strands, 0.84 cm^2 internal diameter surface area). The membranes were characterized by scanning electron microscopy using a LEO 1530 VP instrument (Gottingen, GER) and by thermo gravimetric analysis (TGA) using a Perkin Elmer (Waltham, MA, USA) Pyris instrument.

3.3 Results and Discussion

Scanning electron microscopy (SEM) images at various magnifications with and without CNTs are shown in Figures 3.2a, b, c, d, e and f.

Based on the TGA analysis, it was concluded that the CNIM contained approximately 0.5 weight % of CNTs. It was also observed that the presence of CNTs

enhanced the thermal stability of the membrane by increasing the onset of thermal degradation by as much as 29ºC. This is critical for MD, where relatively high temperatures are used and the higher stability would help slow membrane deterioration. This data is shown if Figure 3.3.

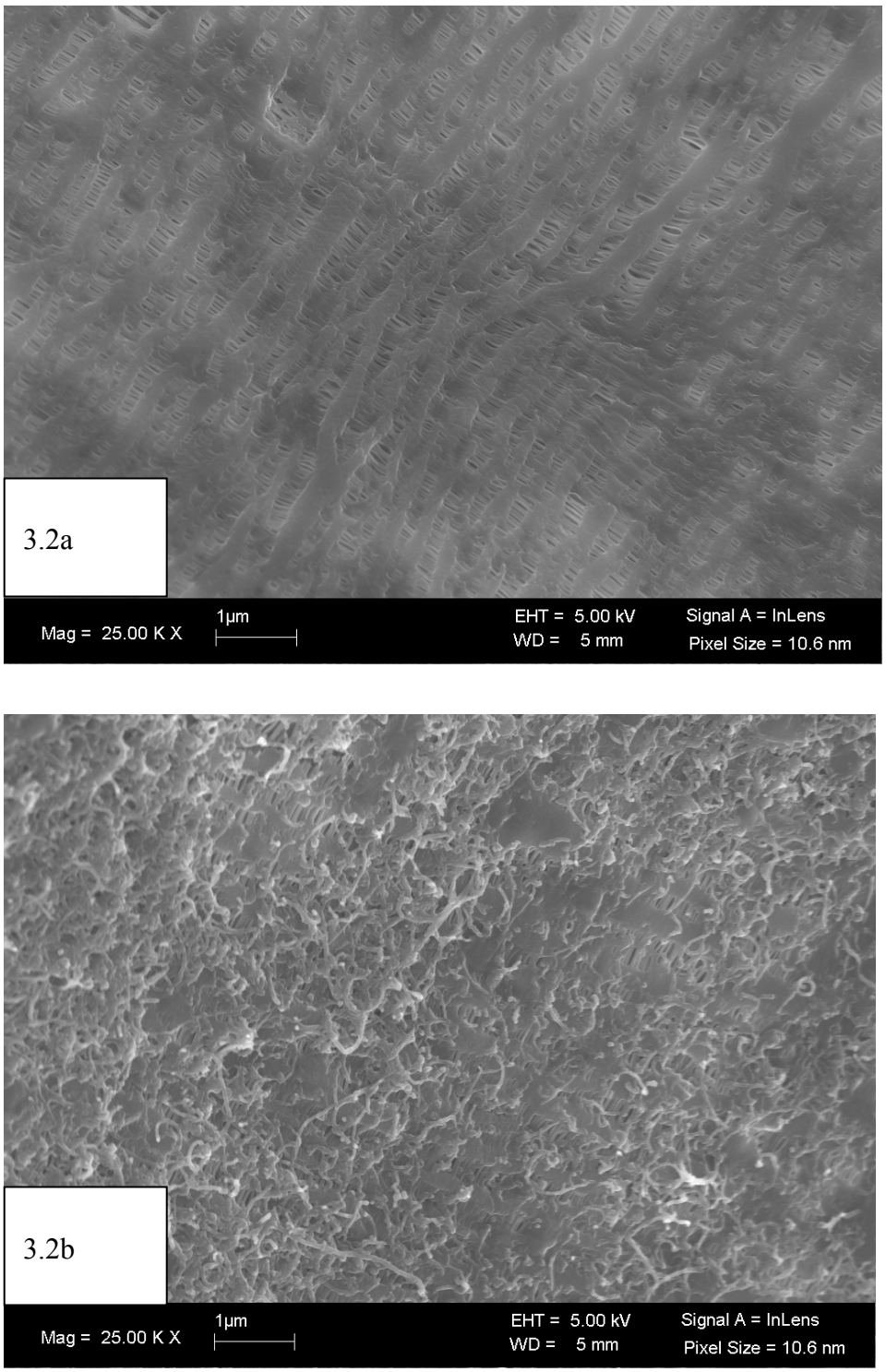

Figure 3.2 Scanning electron micrographs of (a) plain membrane at 25 kX (b) CNIM at 25 kX (c) plain membrane at 70 kX (d) CNIM at 70 kX (e) plain membrane at 100 kX (f) CNIM at 100 kX.

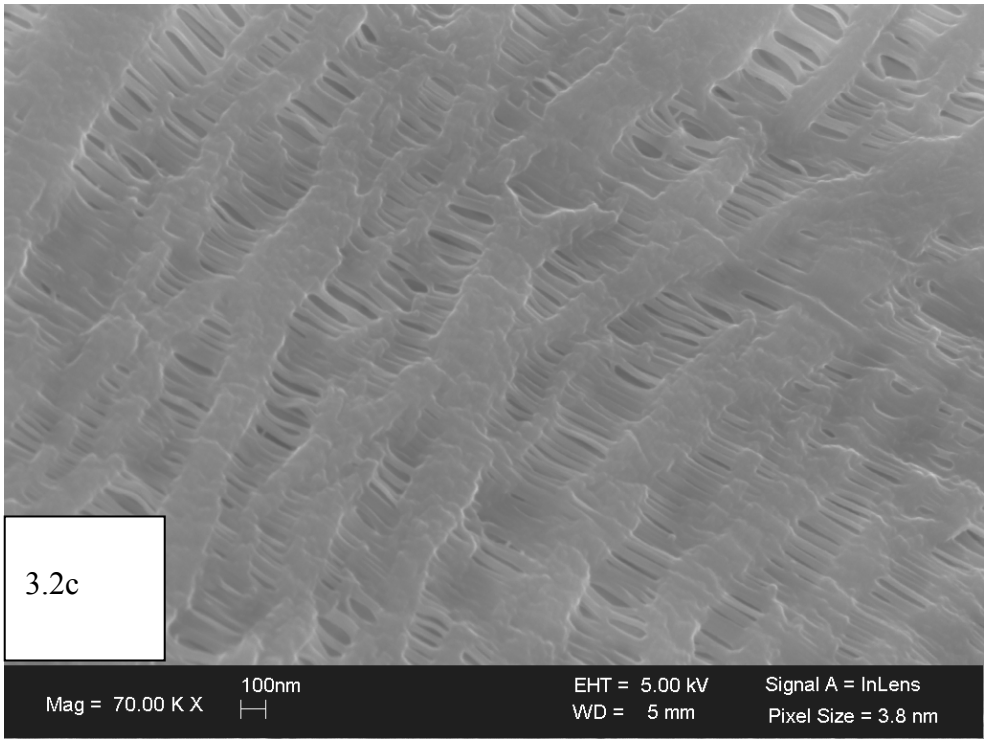

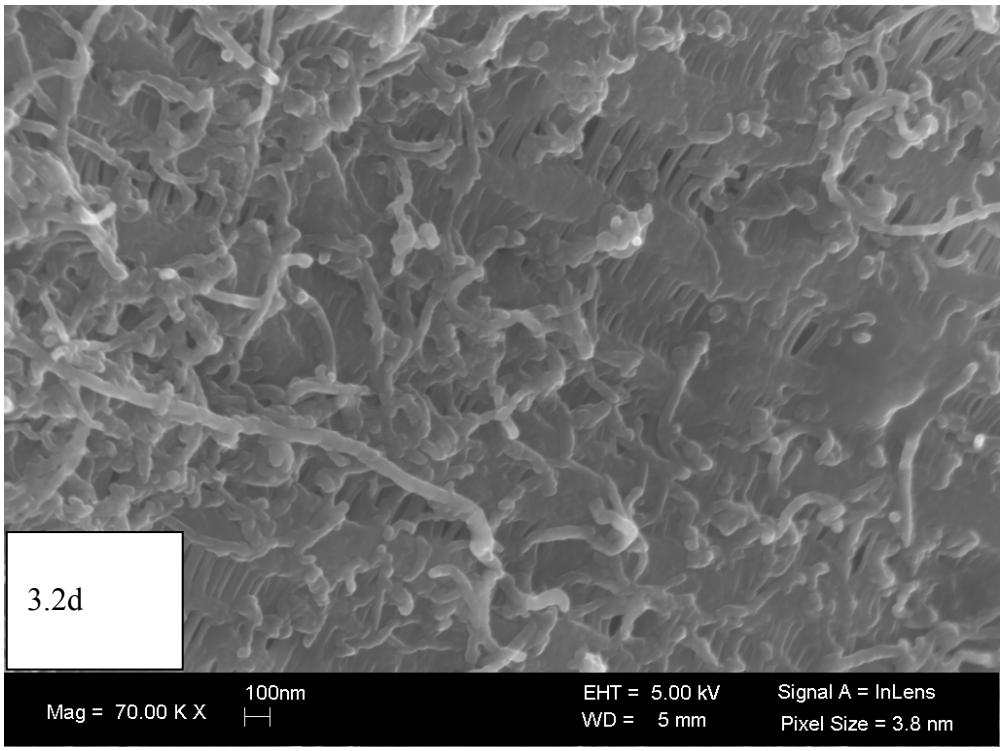

Figure 3.2 Scanning electron micrographs of (a) plain membrane at 25 kX (b) CNIM at 25 kX (c) plain membrane at 70 kX (d) CNIM at 70 kX (e) plain membrane at 100 kX (f) CNIM at 100 kX (Continued).

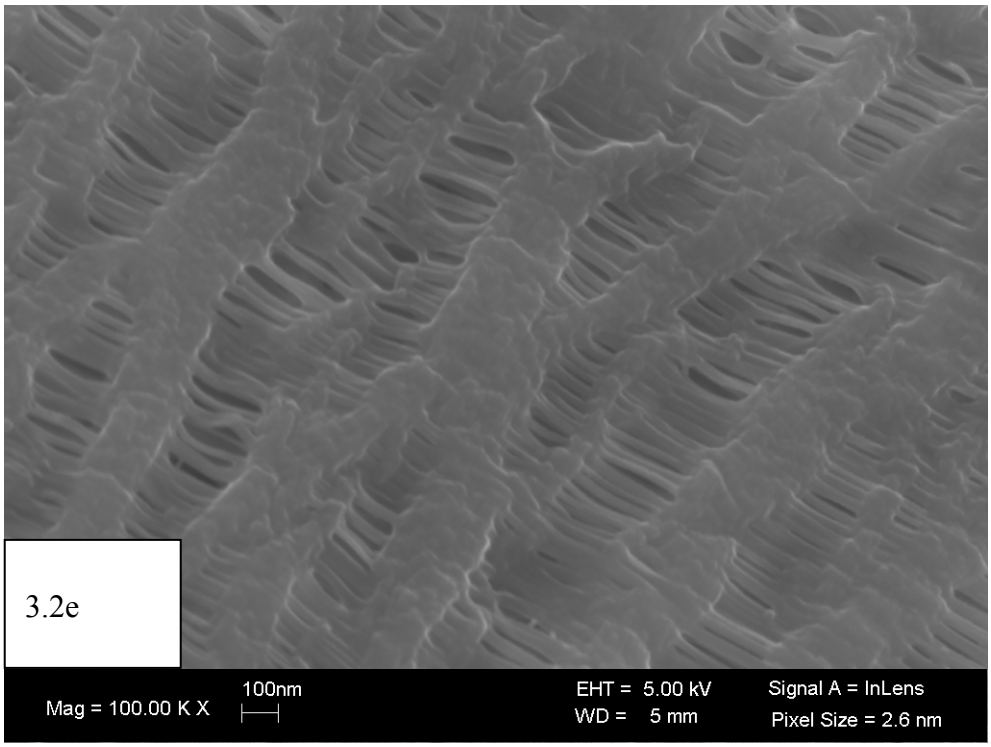

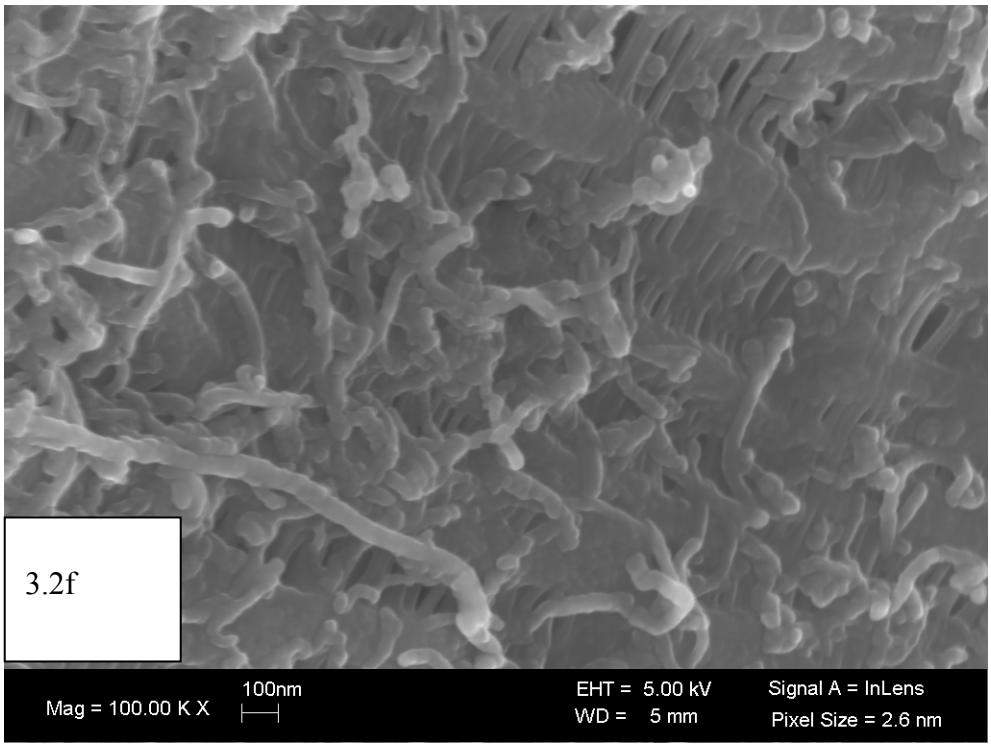

Figure 3.2 Scanning electron micrographs of (a) plain membrane at 25 kX (b) CNIM at 25 kX (c) plain membrane at 70 kX (d) CNIM at 70 kX (e) plain membrane at 100 kX (f) CNIM at 100 kX (Continued).

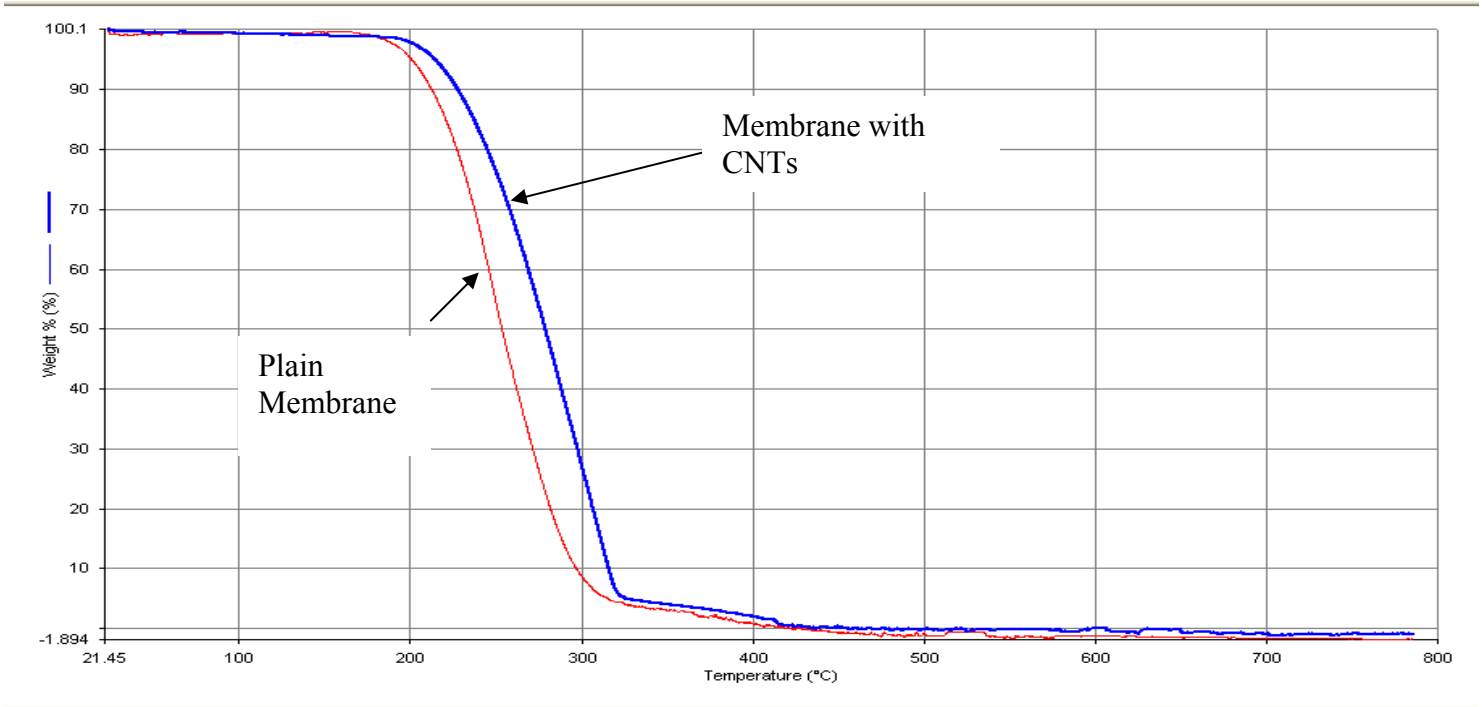

Figure 3.3 Thermal gravitational analysis of plain membrane and CNIM.

3.4 The Preconcentration Effect and Mass Transfer in the Presence of CNTs

The preconcentration effect in MD was quantified as the Enrichment Factor (EF):

$$EF = \left(\frac{C_o}{C_i} \right) \tag{3.4}$$

where, C_o is the outlet analyte concentration and C_i is the inlet concentration. The other important factor was solvent reduction (SR), which was a measure of the amount of water removed and was defined as:

$$\% SR = \frac{V_{i-} V_o}{V_i} X100 \tag{3.5}$$

where, V_i and V_o were in the inlet and outlet volumes.

Another important consideration was the effect of CNTs on mass transfer across the membrane. The water vapor flux, J_w, across the membrane can be expressed as:[148]

$$J_w = k(C^L - C^V) \tag{3.6}$$

where, k is the mass transfer coefficient and C^L and C^V are the liquid and vapor-phase concentrations. The reciprocal of k, the overall resistance to mass transfer[149] depends upon several factors and is expressed as:

$$\frac{1}{k} = \frac{1}{k^L} + \frac{1}{k^M} + \frac{1}{k^V} \tag{3.7}$$

where, $1/k^L$ is the liquid boundary layer resistance, $1/k^M$ is the membrane resistance and $1/k^V$ is the vapor boundary resistance. The liquid boundary layer resistance is dependent on parameters such as feed flow rate, turbulent flow, viscosity, and density. Membrane resistance is a function of the membrane thickness, temperature and the permeability of water vapor through the membrane. Vapor phase boundary layer resistance is affected by surface tension and temperature. A large amount of heat is used to vaporize the solution, this results in a temperature difference between the bulk solution and the membrane surface, causing a temperature polarization. This temperature polarization causes a significant loss in the driving force of the process. The ratio of useful energy for mass transfer of vapors is call the temperature polarization coefficient (TPC) and is the fraction of total thermal driving force that contributes to mass transfer. A higher TPC will increase overall mass transport. A higher feed flow helps to overcome the temperature polarization effect, however the higher pressures involved with pumping the solution faster may cause the pore's break-through pressure to be exceeded and results in pore wetting that prevents further vapor transport.

The flux through the membrane, J, was calculated as:

$$J = \frac{w^p}{tA} \tag{3.8}$$

where, w^p is the total mass of permeate, t is the permeate collection time and A is the membrane surface area. Then, the overall mass transfer coefficient was calculated by:

$$k = \frac{J}{c} \tag{3.9}$$

where k is the mass transfer coefficient and c is the average feed concentration.

Initial optimization of process conditions was carried out using a 5 mg L^{-1} ibuprofen solution in deionized water. Experiments were carried out in the range of 50-100ºC. In both membrane types, there was no measurable increase in concentration at 50ºC (EF was 1.0). At 60ºC, while the plain membrane showed no increase in EF, CNIM showed some preconcentration effect. The maximum enrichment for both membranes types occurred when the aqueous feed solution was at 80ºC. This is shown in Figure 3.4.

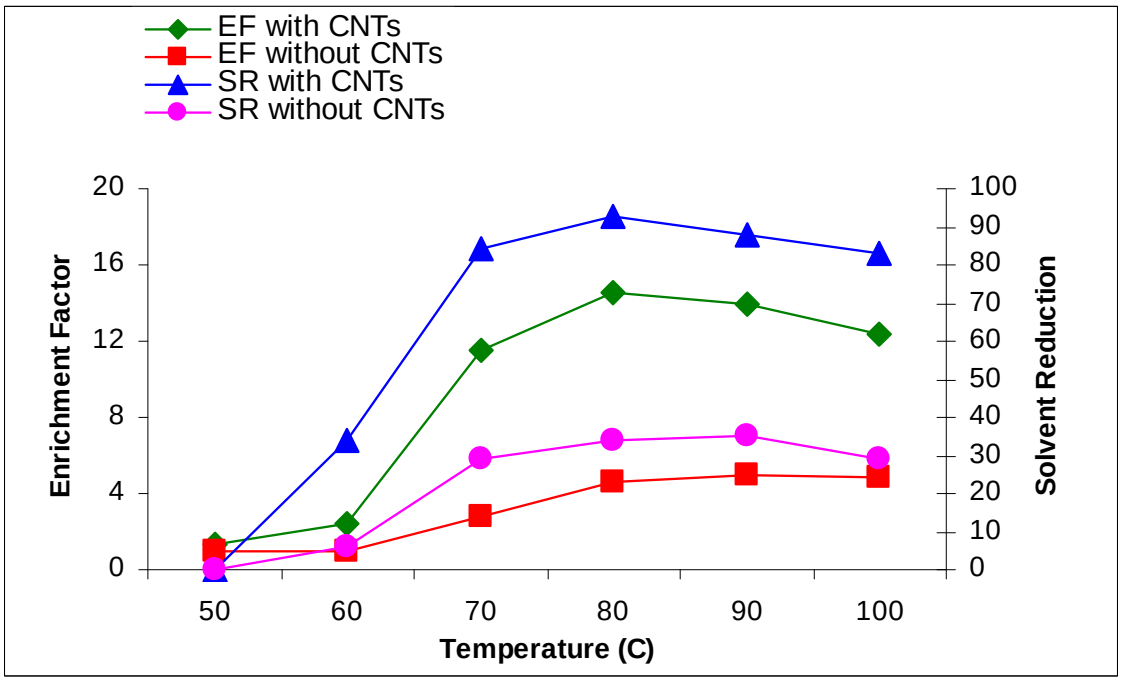

Figure 3.4 EF and SR as a function of temperature at a flow rate of 0.5 ml min^{-1} and 5 mg L^{-1} ibuprofen feed solution.

The mass transfer coefficients at different temperatures are presented in Figure 3.5, and were found to be 4 to 5 times higher in the presence of the CNTs. The effect of temperature on *k* was significantly more pronounced for the plain membrane where the increase was nearly 4 fold in the 50ºC to 80ºC range. This was attributed to an increase in the diffusion coefficient (k^M). In general, while diffusivity in the membrane increased with temperature, the sorption or the partition coefficient decreased. As a result of these two opposing effects, the overall increase in *k* was not as pronounced in the presence of the CNTs.

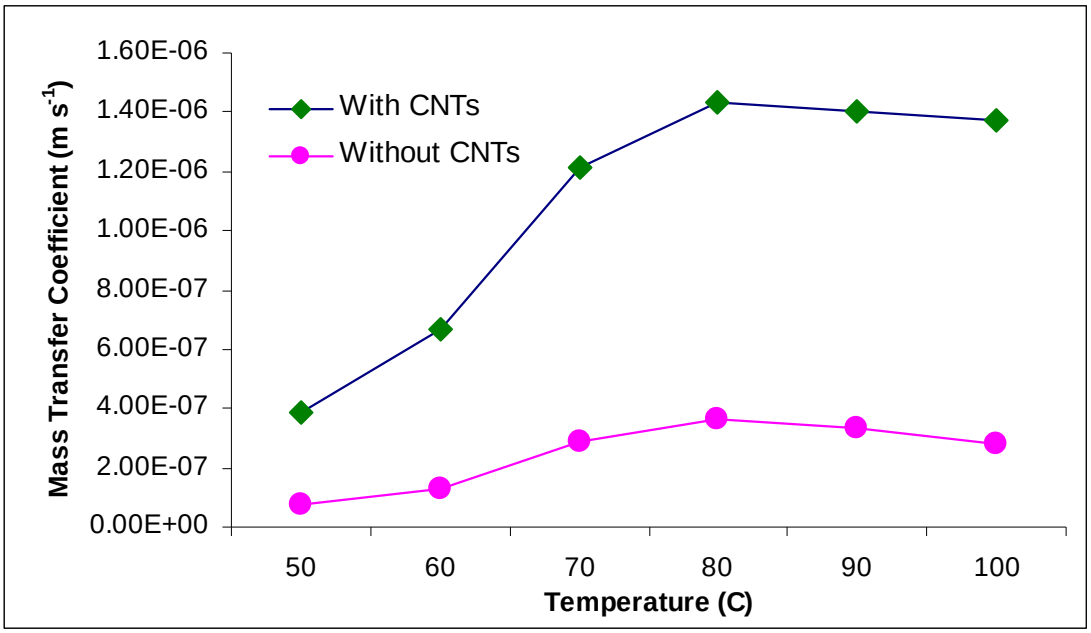

Figure 3.5 Mass transfer coefficient (m/s^{-1}) as a function of temperature.

MD was studied in the flow rate range of 0.25 to 3.0 ml min^{-1}. At 3.0 ml min^{-1}, there was no enrichment for the plain membrane but there was noticeable enrichment and solvent reduction for the CNIM. Maximum enrichment occurred at 0.5 ml min^{-1} for both membranes and there was a leveling out for feed flow rates lower than this. These results are shown in Figure 3.6.

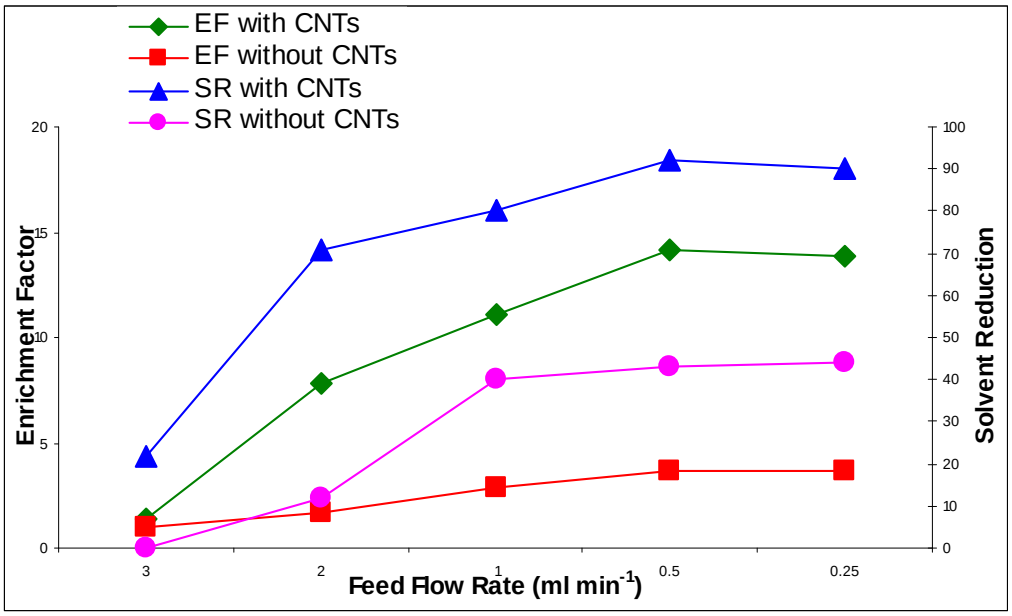

Figure 3.6 EF and SR as a function of feed solution flow rate; at 80°C and 5 mg L^{-1} feed solution, flow rate.

Figure 3.7 shows the effect of flow rate on the mass transfer coefficients. At low flow rates, the overall mass transfer is controlled by diffusion through the boundary layer, while turbulence at high flow rates reduces the boundary layer affects, and at this point the *k* is no longer a function of flow rate. The flattening of the profile was observed for the unmodified membrane but not the CNIM. As the flow rate of feed water was increased from 1.0 to 2.0 mL min^{-1}, *k* in the unmodified membrane increased from 1.12 x 10^{-6} to 1.41 x 10^{-6} ms^{-1}, and stayed more or less constant beyond that point. Interestingly, the overall mass transfer coefficient was less affected by the presence of the CNTs at low flow rates. In general, the presence of the CNTs led to enhanced permeability through the membrane, and mass transfer was not limited by diffusion through the boundary layer even at high flow rates.

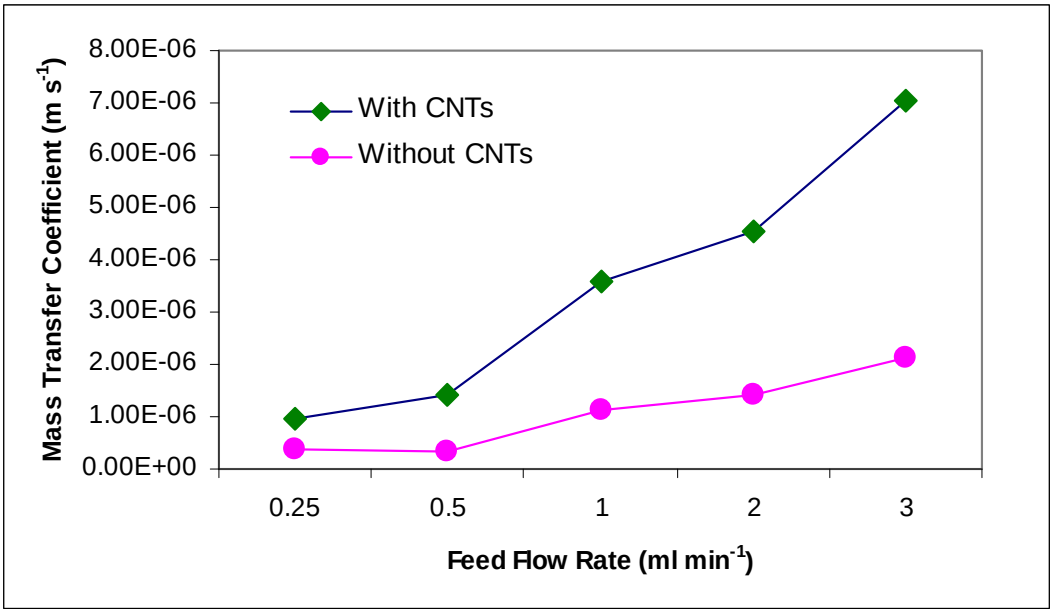

Figure 3.7 Mass transfer coefficient (m/s^{-1}) as a function of feed flow rate.

The effect of inlet concentration in the range of 0.1 to 5 mg L^{-1} was studied at the optimal conditions and these results are shown in Figure 3.8. It was observed that in the range studied, EF and SR did not change significantly with concentration. The mass transfer coefficients were calculated and these were essentially the same at each concentration. Once again, the CNIM consistently showed higher EF and SR than the original membrane, and the mass transfer coefficient was higher by nearly 300%.

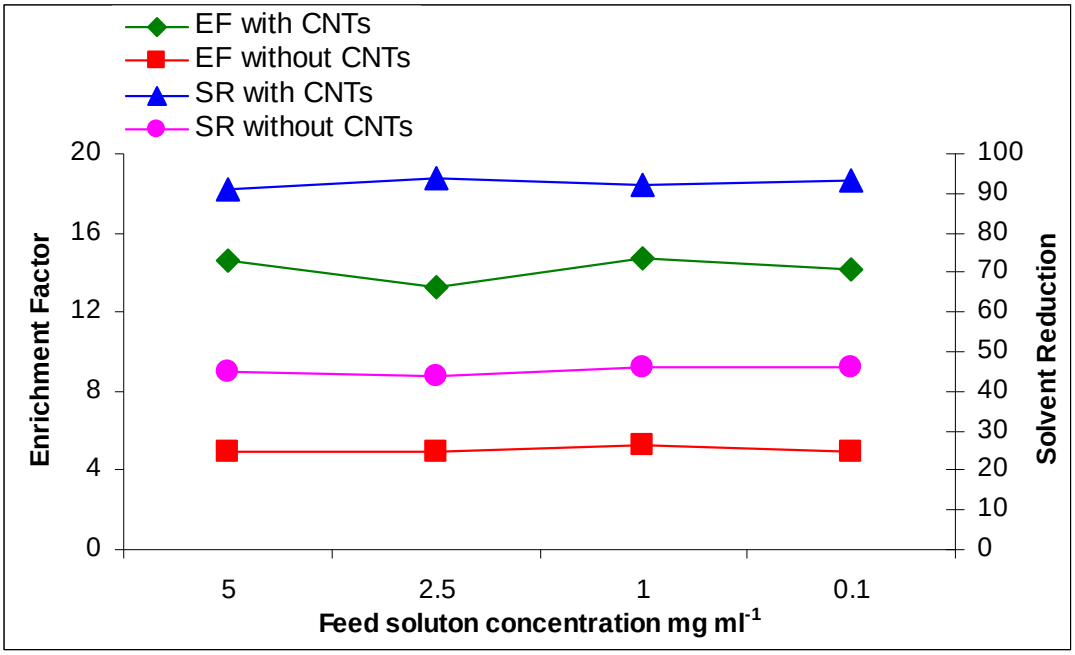

Figure 3.8 EF and SR as a function of inlet concentration of ibuprofen, 80°C and 0.5 ml min^{-1} feed flow.

3.5 Analytical Performance

Other pharmaceutical compounds studied were acetaminophen, diphenhydramine and dibucaine. All compounds showed similar trends as a function of temperature, flow rate, concentration and mass transfer coefficient. EF, SR and mass transfer coefficient was determined for each compound at 0.1, 1.0, 2.5 and 5 mg L^{-1}. All experiments and measurements at all concentrations were measured in triplicate. All results were linear in the concentration range measured. Comparative data is presented in Table 3.1, which represent measurements at 80ºC, 0.5 ml min^{-1} and 1.0 mg L^{-1} concentration. As seen, the EF and SR were significantly higher in the case of CNIM. The EF using the unmodified membrane varied between 3.2 and 5.3, and corresponding values for CNIM were 10.1 to 14.8. The CNIM led to 300% enhancement in EF and up to 270% enhancement in SR. The EF with the plain membrane was similar to that published before for online

concentration using pervaporation, however, the EF using CNIM was found to be significantly higher.

The MD process was highly reproducible with RSD ranging between 2-5%. The calibration curves showed excellent linearity in the range of 0.01 to 5 mg L^{-1} with r^2 greater than 0.995 for all the compounds, so this allowed quantification by the method of external standardization. The detection limits using CNIM at a signal to noise ratio of 3 were 0.003, 0.02, 0.009, 0.005 mg L^{-1} for ibuprofen, acetaminophen, diphenhydramine and dibucaine respectively. Significantly lower detection limits could be achieved by increasing the number of membrane strands in the CNIM module.

3.6 Conclusions

MD via CNIM is an excellent preconcentration method that can be used on-line for the concentration of analytes from an aqueous medium. The approach is universal because it relies on the removal of water rather than the selective permeation of the analytes across a membrane. Further, the technique does not require the use of solvents, so may be considered "green" compared to SPE or liquid-liquid extraction. Conventional MD provided a low enrichment factor, but the introduction of CNTs dramatically increased the performance in terms of enrichment factor, flux and mass transfer coefficients.

Table 3.1 EF, SR and k for Four Pharmaceutical Compounds with Plain Membranes and with CNIM, Feed flow 0.5 ml min^{-1}, 80°C and 1.0 mg L^{-1}

	Plain Membrane			CNIM			% Enhancement by CNIM		
Analytes	EF	%SR	k	EF	%SR	k	EF	SR	k
Ibuprofen	5.3	46	3.35×10^{-7}	14.8	93	1.43×10^{-6}	280	202	427
Acetaminophen	3.2	33	2.41×10^{-7}	10.1	89	1.31×10^{-6}	316	270	543
Diphenhydramine	4.8	45	3.50×10^{-7}	13.9	92	1.40×10^{-6}	290	204	400
Dibucaine	3.5	37	2.88×10^{-7}	11.8	95	1.43×10^{-6}	337	257	497

CHAPTER 4

CARBON NANOTUBE ENHANCED MEMBRANE DISTILLATION FOR ON-LINE PRECONCENTRATION OF TRACE PHARMACEUTICALS IN POLAR SOLVENTS

4.1 Introduction

The objective of this work was to determine if enhanced MD could be applied as an preconcentration technique for monitoring trace impurities by the selective removal of organic solvents. Of particular interest is the monitoring of drug molecules in methanol, which is a common solvent used in many pharmaceutical manufacturing operations.

4.2 Experimental

Two new membrane modules were prepared (one with plain membrane and the other with CNIM) and were similar to those used in Chapter 3. Experimental conditions were the same as before except that methanol was used in place of water for all experimental work.

4.3 Results and Discussion

Process optimization was carried out using a 5 mg L^{-1} ibuprofen solution in methanol. The results of feed solution temperature at constant flow are shown in Figure 4.1.

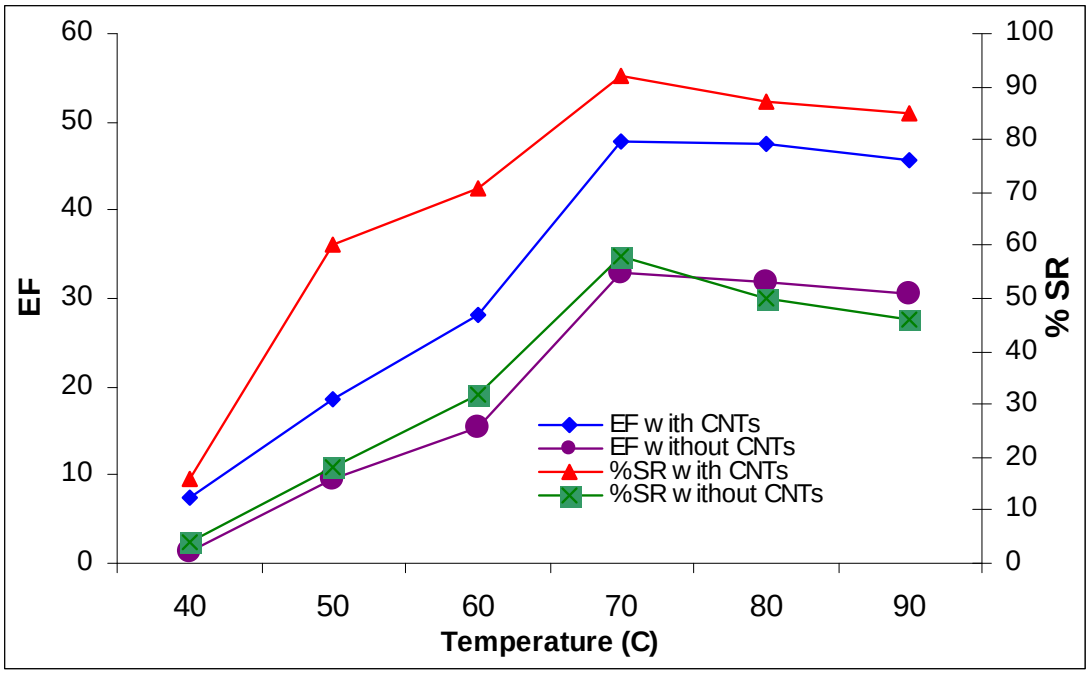

Figure 4.1 EF and SR as a function of temperature at a flow rate of 0.75 ml min^{-1} and 5 mg L^{-1} ibuprofen feed solution.

Experiments were carried out in the range of 40- 90ºC. Maximum enrichment was reached at a temperature of 70ºC for both the CNIM and the plain membrane. The CNIM consistently showed higher EF than the plain membrane. For example, at 70ºC, EF and SR were 159% and 146% higher with the CNIM. Significantly higher EF could be accomplished using the CNIM at a lower temperature, implying that the same preconcentration could be carried out under cooler conditions.

The mass transfer coefficients at different temperatures are presented in Figure 4.2. The CNIM had significantly higher mass transfer coefficients at all temperatures. The effect of temperature on k was significantly more pronounced for the plain membrane in the 40ºC to 80ºC range. This was attributed to an increase in the membrane diffusion coefficient.

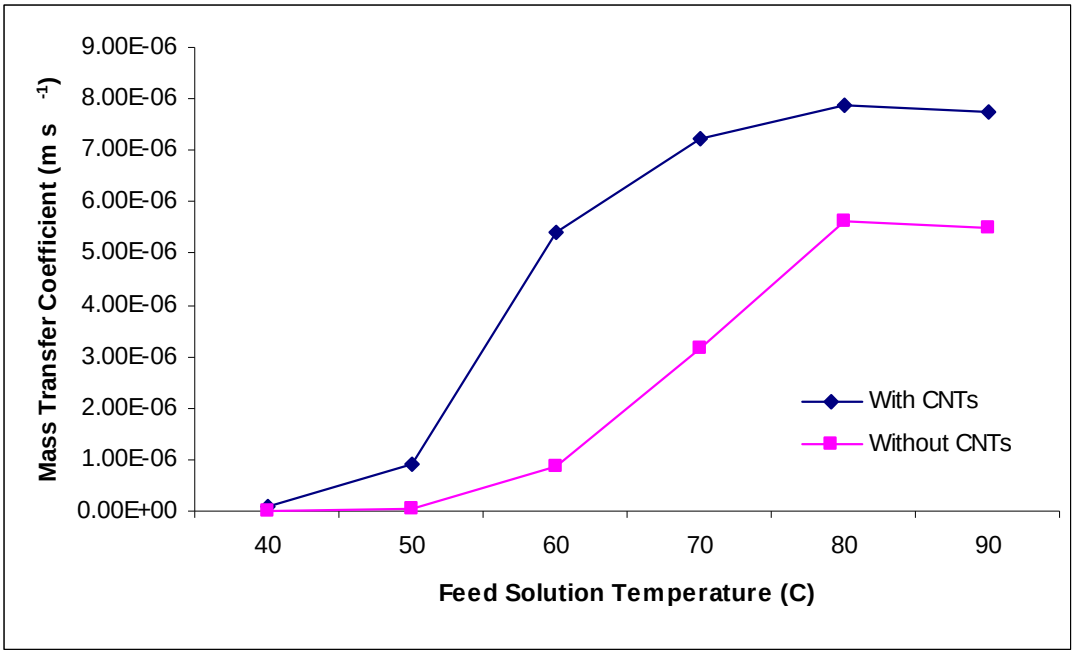

Figure 4.2 Mass transfer coefficient (m/s^{-1}) as a function of temperature.

MD was studied in the flow rate range of 0.5 to 1.0 ml min^{-1}. EF began to reduce beyond 0.75 ml min^{-1} for both the membranes, which was attributed to lower residence time and less time for mass transfer. The data is presented in Figure 4.3. Once again, for all measurements, EF and %SR for the CNIM was higher than the plain membrane. In fact, the best EF and % SR values for the plain membrane were lower than the worst values obtained for CNIM (1.0 ml min^{-1} feed flow).

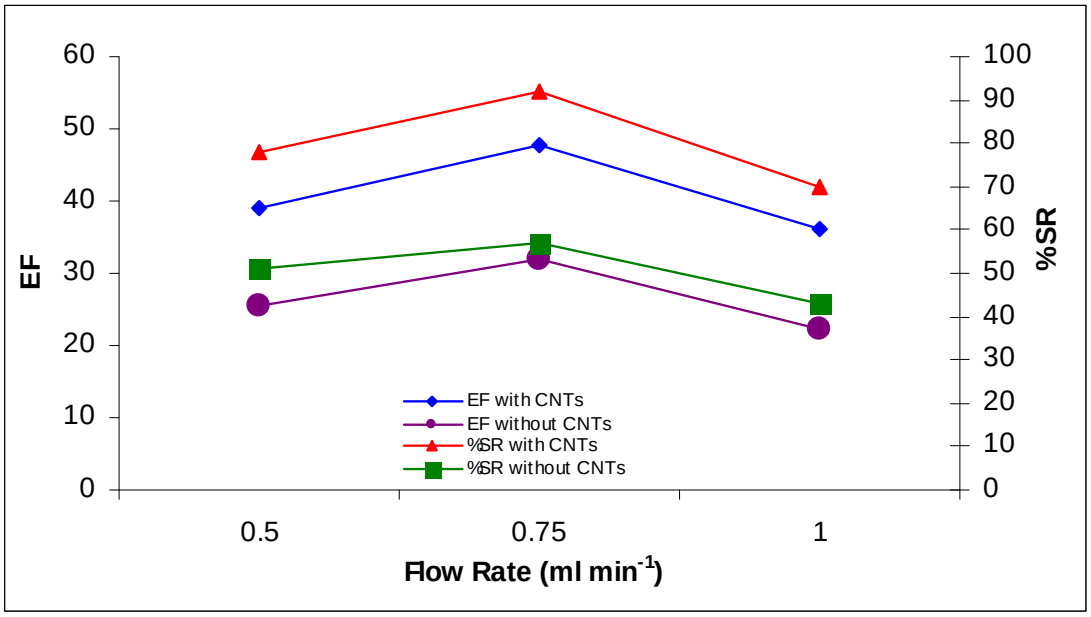

Figure 4.3 EF and SR as a function of feed solution flow rate; at 70°C and 5 mg L^{-1} ibuprofen feed solution.

Figure 4.4 shows the effect of flow rate on the mass transfer coefficients. There was a flattening of the profile with the plain membrane but not for the CNIM. As the flow rate of bulk feed was increased from 0.5 to 0.75 mL min^{-1}, k in the unmodified membrane increased from 1.53 x 10^{-6} to 2.14 x 10^{-6} ms^{-1}, then stayed constant. This was attributed to boundary layer diffusion. The presence of the CNTs led to enhanced permeability through the membrane, and mass transfer was not limited by diffusion through the boundary layer at high flow rates.

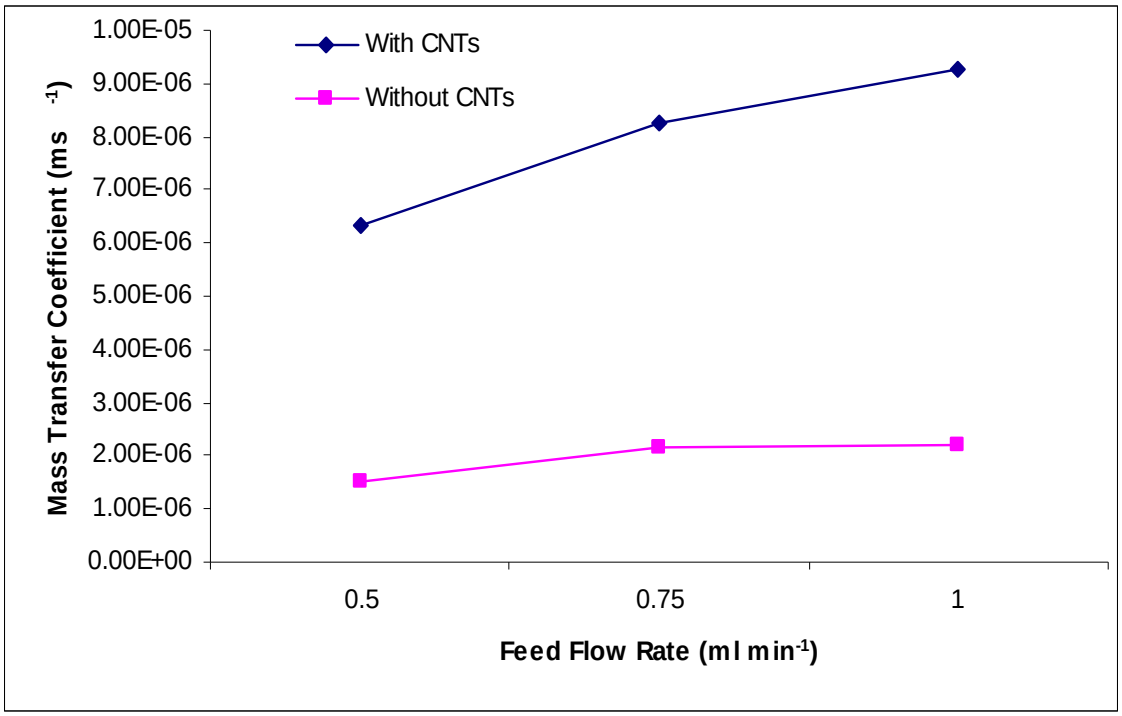

Figure 4.4 Mass transfer coefficient (m/s^{-1}) as a function of feed flow rate.

The effect of inlet concentration in the range of 0.1 to 50 mg L^{-1} was studied at the optimal conditions and these results are shown in Figure 4.5. It was observed that in the range studied, EF and SR did not change significantly with concentration. The mass transfer coefficients were calculated, and these were relatively constant independent of the concentration. Once again, the CNIM consistently showed higher EF, SR and mass transfer coefficients than the original membrane.

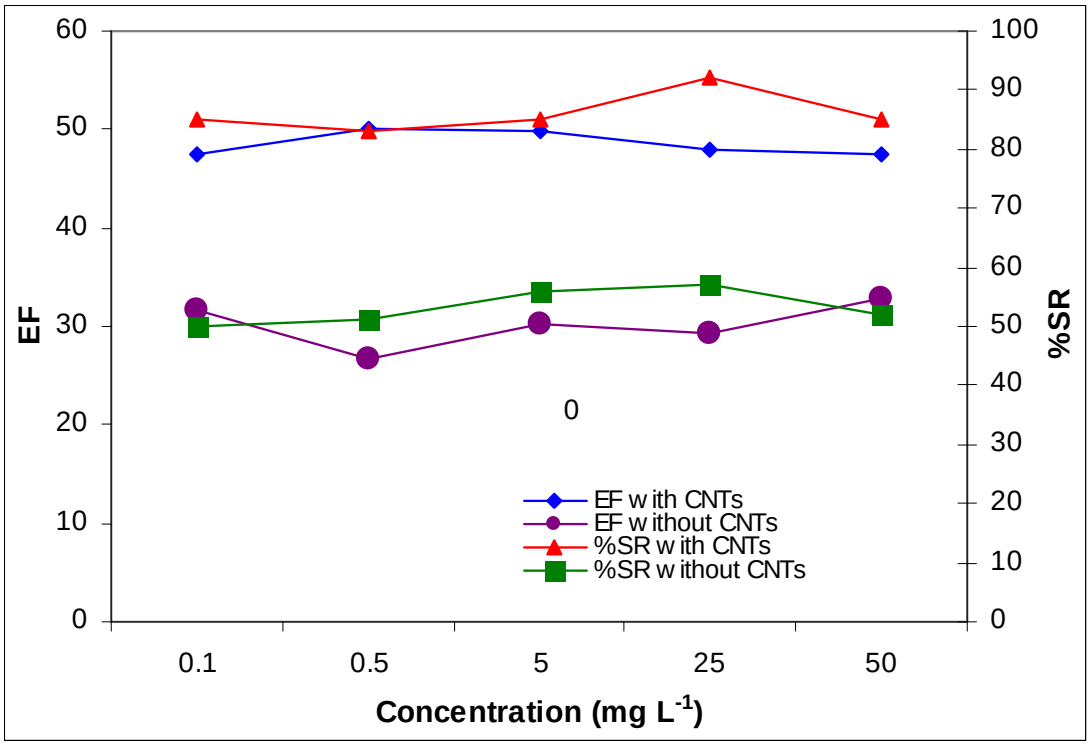

Figure 4.5 EF and SR as a function of inlet concentration of ibuprofen, 70°C and 0.75 ml min^{-1} feed flow.

4.4 Analytical Performance

Other pharmaceutical compounds, namely, acetaminophen, diphenhydramine and dibucaine were studied. All compounds showed similar trends as a function of temperature, flow rate, concentration and mass transfer coefficient. EF, SR and mass transfer coefficient were determined for each compound at 0.1, 0.5, 5, 25 and 50 mg L^{-1}. All experiments and measurements at all concentrations were measured in triplicate. All results were linear in the concentration range measured. The results are presented in Table 4.1, which represent measurements at 70ºC and 0.75 ml min^{-1} feed flow rate and 0.5 mg L^{-1}. As seen, the EF and SR were significantly higher in case of CNIM. The EF using the plain membrane varied between 6 and 29, while CNIM showed 13 to 48. The CNIM led to 160 to 260% enhancement in EF and up to 161% enhancement in SR

The MD process was highly reproducible with RSD ranging between 2-4%. The calibration curves showed excellent linearity in the range of 0.1 to 50mg L^{-1} with an r^2 of greater than 0.992 for all the compounds, so this allowed quantification by the method of external standards. The detection limits were 0.001, 0.009, 0.004, 0.003 ug ml^{-1} for ibuprofen, acetaminophen, diphenhydramine and dibucaine respectively. Significantly lower detection limits can be achieved by increasing the number of membrane strands, which would allow for greater loading of CNTs and a corresponding increase in solvent reduction.

4.5 Conclusions

MD via CNIM is an excellent preconcentration method for polar organic solvents that can be used on-line. The approach is an alternate to conventional distillation and is universal because it relies on the removal of solvent rather than the selective permeation of the analytes across a membrane. Conventional MD provided a low enrichment factor, but the introduction of CNTs dramatically increased the performance in terms of enrichment factor, flux and mass transfer coefficients.

Table 4.1 EF and %SR for Four Pharmaceutical Compounds (EF and %SR from Measurements at 0.5 mg L^{-1})

Analytes	EF			%SR		
	CNIM	Plain	%Enhancement in CNIM	CNIM	Plain	%Enhancement in CNIM
Ibuprofen	48	29	166	92	57	161
Acetaminophen	13	6	217	80	55	145
Diphenhydramine	29	15	193	92	64	144
Dibucaine	37	14	264	95	61	156

CHAPTER 5

WATER DESALINATION USING CARBON NANOTUBE ENHANCED MEMBRANE DISTILLATION

5.1 Introduction

Water is an essential resource for ensuring human health, and the lack of suitable water to meet the daily needs for human consumption is a reality. The importance of water to life on earth can not be too highly stated. On a global scale water quality is being impaired or threatened by many factors, including industrial discharges, rainwater runoff and agricultural activities. Drinking water quality has a huge direct impact on public health. The lack of sufficient quantities of water suitable for human consumption is a growing problem and is recognized by agencies such as the World Health Organization (WHO) as the most serious threat to the health of global populations.[150] This limited supply of drinking water is competing with increasing industrial and agricultural demands for water.

Even in areas where there is sufficient rainfall, the low quality of the stored water often prevents its use. About 20% of the world's population resides in areas where water is physically scarce. For a significant portion of the world, there is lack of adequate infrastructure to ensure water quality. Poor water quality can lead to increased incidence of diseases such as dysentery and typhus. The lack of suitable quality water has led to an increase in the use of both human and industrial waste water for agricultural purposes. When food from this practice is consumed, it raises the risk of both microbial and chemical contamination.

Countering this, there is a potentially unlimited supply of water for human, industrial and agricultural use contained in the earth's seas and oceans. Unfortunately,

the high salt content of seawater prevents its use. Salinity refers to the concentration of salt in water. The average salinity of the world's oceans is about 34,000 mg L^{-1}, consisting primarily of sodium chloride (88%), magnesium sulfate (11%) with the remainder divided between various other inorganic salts.[151]

It has long been hoped that economically viable technologies can be developed that would allow for removal of salt. While there are existing technologies that can remove these high salt levels in water, they are expensive and technically difficult to operate and maintain. These are also prone to failure due the corrosive effects of the salts. Currently the most commonly used process for seawater desalination is reverse osmosis (RO).

RO is a process by which water is deionized by using pressure.[152] In natural osmotic systems, water flows across a semi-permeable membrane from areas of low salt content to areas of high salt content, or simply fresh water moves to dilutes salt water. The functioning of the human kidney is an example of a natural osmotic system. In RO, the flow is reversed. By applying a high enough pressure (the osmotic pressure) water of no or low salt content will move from a high salt content water across the membrane. The low salt content water is collected as permeate on the far side of the membrane and the remaining feed solution (concentrate) has a higher salt content than the original solution. Whereas MD is a vapor pressure-temperature driven process, RO is a pressure driven process. Because of the relatively high pressures (300-600 psi) involved in RO, specialized equipment is needed, such as pressure vessels to contain the membranes and multi-stage pumps.

Most applications using RO have been with "brackish" water, which is defined as water that has a lower salinity than seawater, but has a higher salt content than is suitable

for human consumption. According to the US EPA regulations in the Safe Drinking Water Act (SDWA), the salt content of drinking water is a secondary health characteristic and it is recommended there be no more than 100 mg L^{-1} of total salt.[153] Brackish water typically will contain somewhere between 100 to 10,000 mg L^{-1} of total salinity. Wide use of desalination of brackish waters is found in the eastern Caribbean islands where water in mangrove swamps is purified.

RO is used to desalinate brackish water because the lower salt content allows for substantially lower operating costs. This is primarily due to lower pressure requirements needed to generate the required osmotic pressure. This in turn lowers the electrical load needed for the pumps used in the process. The lower dissolved solids load in brackish water decreases the corrosion and scaling effects associated with seawater desalination. This makes the overall RO process more efficient from both an operation and cost standpoint as compared to desalinating seawater. However, in terms of absolute volumes and available supply, there is infinitely more seawater available than brackish water.

While significant work has been completed investigating the use of MD with seawater desalination, to date there has been little or no investigation of MD's application to the desalination of brackish water. The objective of this research was to study the effect of CNIM on the enhancement of desalination efficiency of brackish water via membrane distillation (MD).[154]

5.2 EXPERIMENTAL DETAILS

The experimental system is shown in Figure 5.1. Two new modules were prepared, the same as those used in Chapters 3 and 4. The salt mixture used in experiments contained 88% NaCl and 12% $MgSO_4$. The solutions tested ranged from 10 to 34,000 mg L^{-1}. The water to be treated was pumped through the module using a HPLC pump. The solution traveled through a heat exchanger which allowed it to be heated to the desired temperature. As the solution traveled up the module, the permeate was discharged through the drain port and collected in a vacuum trap. The ionic strength of the original solution, the permeate and the concentrate were measured using an Oakton EC Testr 11+ multi range conductivity meter. All experiments were repeated in triplicate and the relative standard deviation of these measurements were found to be less than 5%.

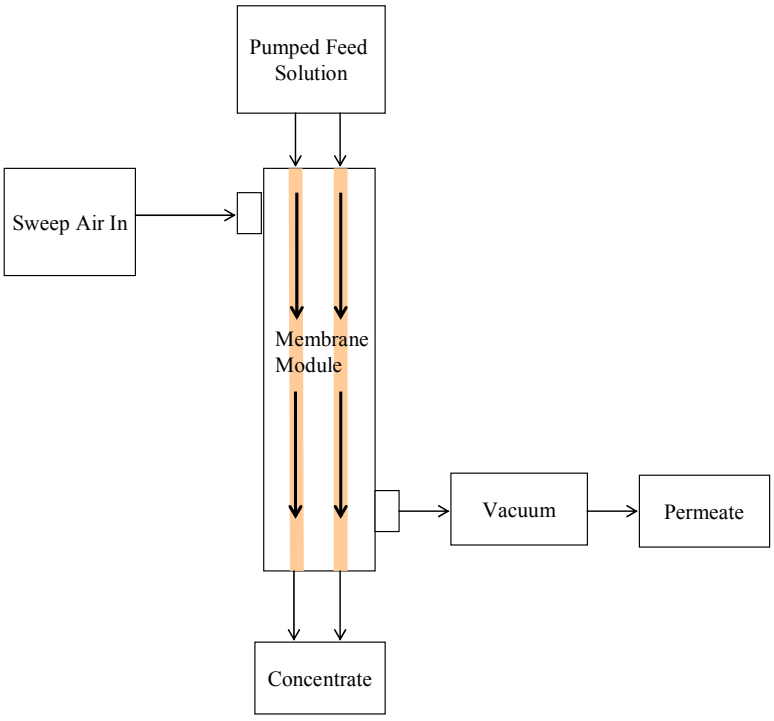

Figure 5.1 Schematic diagram of the experimental set up.

5.3 Results and Discussion

MD experiments were carried out in the range of 60-100ºC. For both membrane types, the salt reduction and flux increased with temperature up to 80º C. There was a leveling off and even slight reduction at higher temperatures. This data is shown is Figure 5.2.

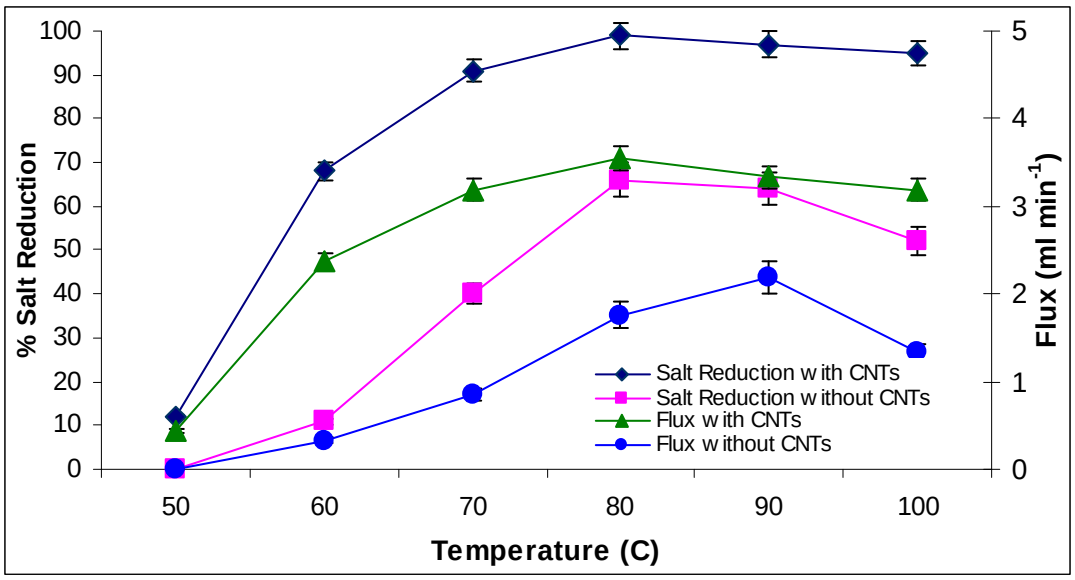

Figure 5.2 Effect of temperature on salt reduction and flux at a feed flow rate of 0.5 ml min^{-1}.

The absolute level of salt reduction and flux per cm^2 of membrane was higher for CNIM at all temperatures. The incorporation of CNTs generated higher salt reduction and flux at significantly lower temperatures. The effect was most pronounced at lower temperatures. For example at 60^o C and 0.5 ml min^{-1} feed flow, the salt reduction using CNIM was 6 times higher and was nearly the same as that accomplished at 90^o C using the conventional membrane. Both salt reduction and flux reached their peaks at 80^o C when the CNIM was used. The data demonstrates that CNIM can provide significantly higher eco-efficiency, because more pure water generation can be carried out at a significantly lower temperature.

Desalination as function of flow rate is shown in Figure 5.3 when feed solution temperature was at 80°C.

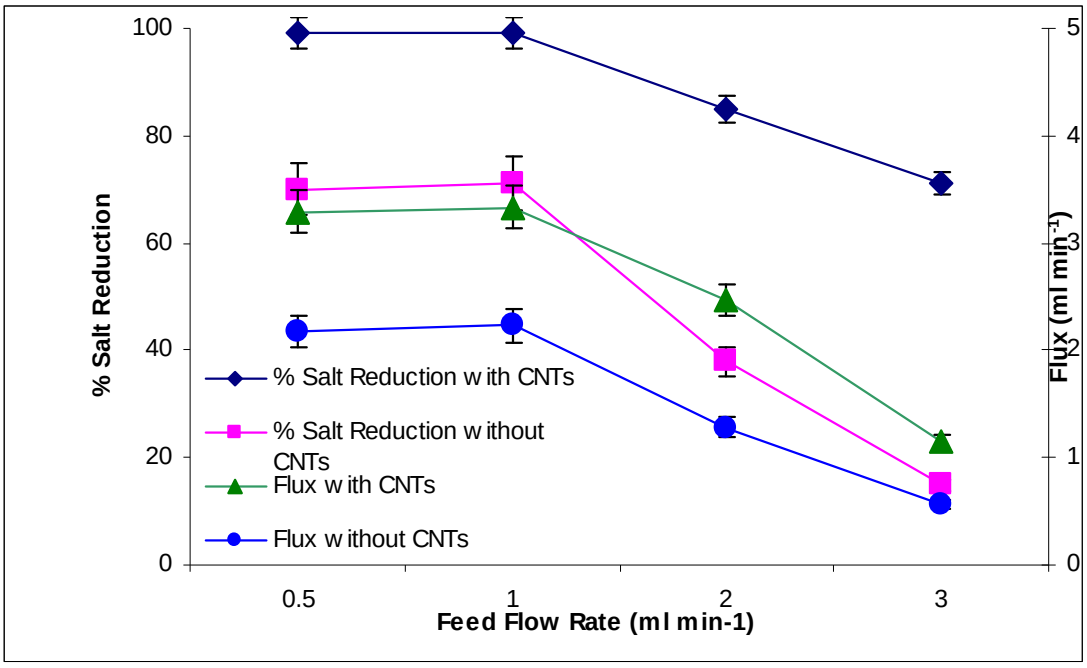

Figure 5.3 Effect of flow rate on salt reduction and flux at 80°C.

In the flow rate range studied, for both membrane types the salt reduction and flux per cm^2 of membrane decreased with increasing flow rate. Compared to the conventional membrane, the CNIM demonstrated significantly higher flux and salt reduction at all feed flow rates. Flux increased by as much as two times in the presence of CNTs and salt reduction increased by almost as much as five times. This is attributed to some of the reasons mentioned above, especially the fact that the CNTs serve as sorbent sites for vapor transport while rejecting the liquid water due to its high hydrophobicity. Salt reduction improved at all flow rates, ranging from 1.39 to 4.73 times higher. The ionic radius of Na^+ and Cl^- are 1.02 and 1.81 Å respectively.[155] It is well known that during reverse osmosis, water clusters exceeding four molecules can transport salt ions through

the polymeric membrane.[156] Since the pores here are significantly larger (0.04 micron), the salt permeation in the membranes occurs mainly due to the entrainment of fine liquid droplets in the vapor phase. Therefore, it is concluded that the enhancement in salt reduction in the presence of the CNTs is due to the relatively higher vapor flux and rejection of water molecules due to higher hydrophobicity. The higher flux and salt reduction have practical ramifications because they lead to significantly higher efficiency processes. Higher salt reduction can be attained at higher flow rates thus requiring less membrane material and energy per unit of water treated.

It is well known that salt reduction in membrane processes decreases with increased salt concentration,[157,158] this is primarily due to the decrease in water activity as concentration increases. This was measured as a function of salt concentration and the data is presented in Table 5.1. The measurements were carried out at a flow rate of 1 ml min^{-1} and 80ºC. These measurements were carried out in triplicate and represent a relative standard deviation of less than 5%. The results showed a substantial decrease in flux (25%) for the plain membranes as the salt concentration was increased from 10 to 34,000 mg L^{-1}. This phenomenon has been reported before.[159,160] On the other hand, the CNIM showed no decrease in flux, most likely due to the hydrophobic nature of the CNTs, which prevented the liquid phase penetration into the membrane. Also, the salt reduction capability of CNIM was significantly higher at all concentrations. The salt reduction varied from 99% to 15%, while in the plain membrane it was 71% to 1%. This indicates the CNIM was less susceptible to salt bleed-through than the standard membrane. Once again this is attributed to the CNIM's ability to selectively allow the passage of water vapor.

The mass transfer coefficients at a flow rate of 0.5 ml min^{-1} and different temperatures are presented in Figure 5.4, and were found to be 2 to 6 times higher in the presence of the CNTs. The effect of temperature on *k* was significantly more pronounced for the plain membrane where the increase was nearly 6 fold in the 60ºC to 80ºC range. This was attributed to an increase in the diffusion coefficient. In general, while diffusivity in the membrane increases with temperature, the sorption or the partition coefficient decreased. As a result of these two opposing effects, the overall increase in *k* was not as pronounced in the presence of the CNTs.

Figure 5.5 shows the effect of flow rate (at 80°C) on the mass transfer coefficient. At low flow rates, the overall mass transfer is controlled by diffusion through the boundary layer. Turbulence at high flow rates may reduce the boundary layer effects, and at this point *k* is no longer a function of flow rate. The flattening of the profile was observed for the unmodified membrane but not the CNIM. As the flow rate of feed water was increased from 0.5 to 1.0 mL min^{-1}, *k* in the unmodified membrane increased from 2.78×10^{-6} to 5.63×10^{-6} m/s, and stayed more or less constant beyond that point.

Table 5.1 Salt Reduction and Flux at Different Feed Concentrations, All Measurements at 80°C and at a Feed Flow Rate of 0.5 ml min^{-1}.

	Membranes with CNTs		Membranes without CNTs	
Feed solution concentration (mg/L)	%salt reduction	total flux ($ml/cm^2/min$)	% salt reduction	total flux ($ml/cm^2/min$)
10	99	3.23	71	2.24
100	93	3.19	56	1.90
1,000	32	3.28	13	2.00
10,000	27	3.05	2	1.86
34,000	15	3.09	1	1.67

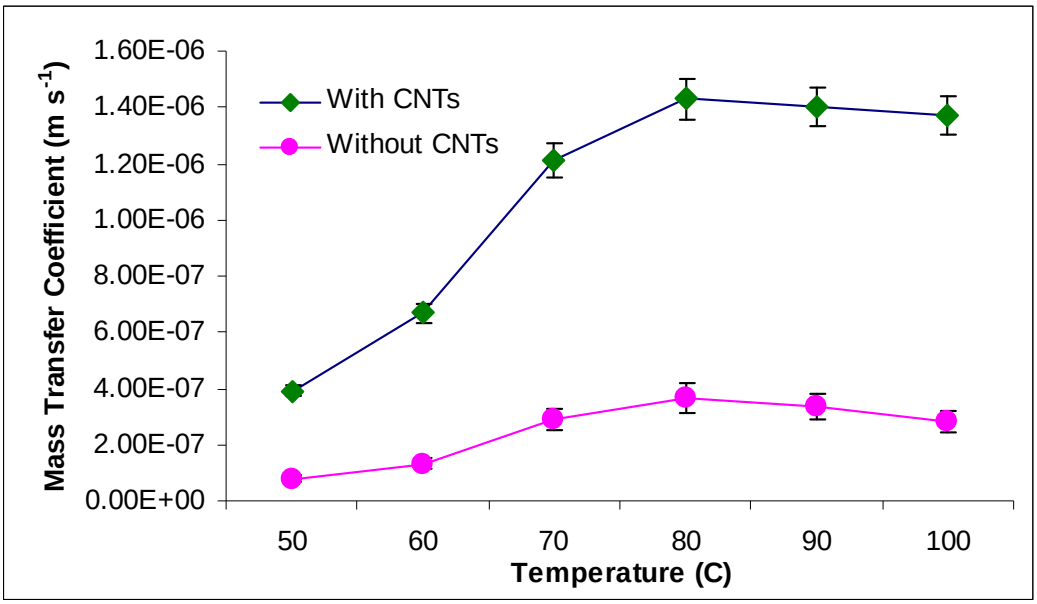

Figure 5.4 Mass transfer coefficients as a function of temperature at a feed flow rate 0.5 ml min $^{-1}$.

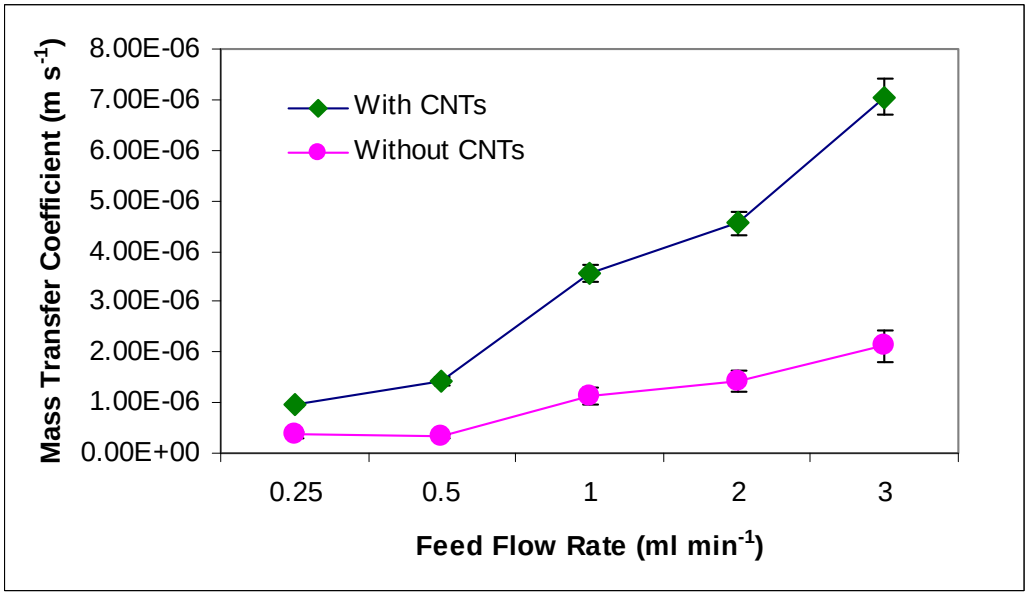

Figure 5.5 Mass transfer coefficients as a function of flow rate at 80°C.

Interestingly, the overall mass transfer coefficient was less affected by the presence of the CNTs at low flow rates and the difference increased with flow rate. At a flow rate of 0.5 mL min^{-1}, the mass transfer coefficient of the CNIM was 1.41 times higher than the unmodified membrane, but increased to 2.72 times higher at 3 mL min^{-1}. In general, the presence of the CNTs led to enhanced permeability through the membrane, and mass transfer was not limited by diffusion through the boundary layer even at high flow rates. The mass transfer coefficients as a function of inlet salt concentration at 80°C and 0.5 ml min^{-1} are presented in Figure 5.6. As expected, the values of *k* decreased with concentration, although they were consistently higher in the presence of CNTs. As compared to the plain membrane, in the salt concentration range of 10 to 10,000 mg L^{-1}, the mass transfer coefficients for the CNIM were higher by a factor of 1.4-3.5. At an inlet salt concentration of 34,000 mg L^{-1}, the CNIM represented a salt reduction that was higher by a factor of 15. This indicates that even at this extreme concentration, the CNIM selectively allowed the passage of water vapor and minimized salt permeation.

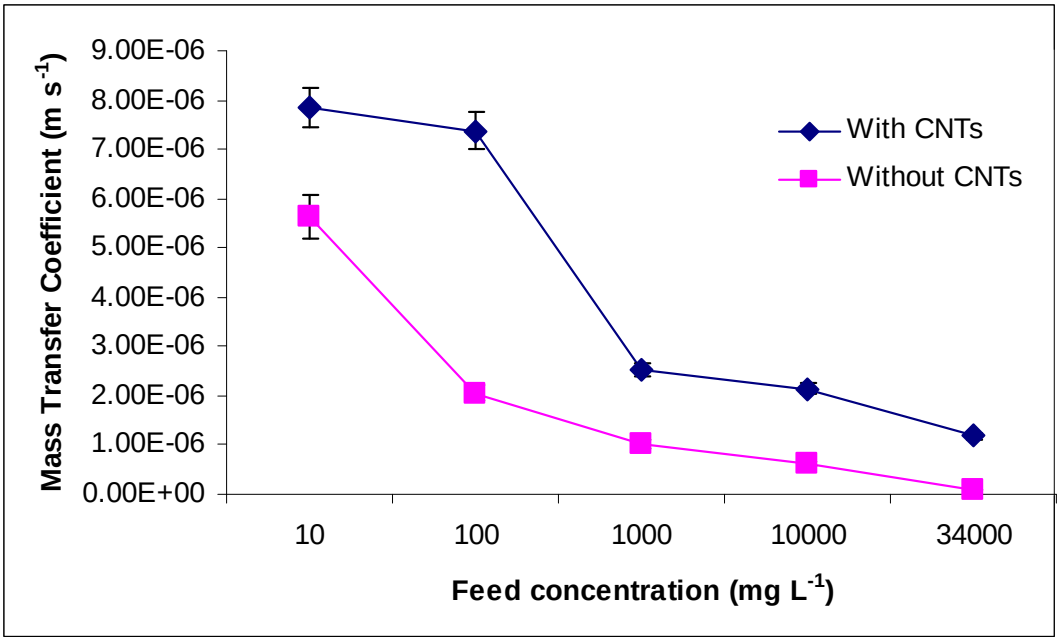

Figure 5.6 Mass transfer coefficients as a function of concentration at a flow rate of 0.5 ml min $^{-1}$ and temperature of 80°C.

5.4 Conclusions

The advantages of CNIM compared to conventional MD include significantly higher flux and salt reduction for a wide range of salt concentrations up to the equivalent of sea water. Another advantage is that the CNIM can facilitate membrane distillation at a relatively lower temperature, higher flow rate and salt concentration. Compared to a plain membrane, the CNIM demonstrated the same level of salt reduction at a 20°C lower temperature, and at a flow rate that was six times higher. Together these lead to a more efficient process which could potentially make MD economically competitive with existing desalination technologies.

CHAPTER 6

CONCENTRATION OF TRACE INORGANICS IN AQUEOUS STREAMS USING CARBON NANOTUBE ENHANCED MEMBRANE DISTILLATION

6.1 Introduction

The primary investigations of MD into water purification applications have involved bulk water removal from high solids content solutions, containing several thousand mg L^{-1} of a compound . Little or no work has been completed investigating the use of MD to remove or concentrate low levels of inorganic impurities in water. This study compares the MD performance of the plain and CNIM membrane types with their ability to concentrate or remove low levels of inorganic impurities from an aqueous stream.

High purity water treatment is a variety of processes for removing pollutants from water, or conversely as a means to concentrate trace levels of valuable materials that may be contained in a water supply. Many waters would be suitable for human consumption except for the presence of low levels of a contaminant (for example chrome or barium). Once these are removed, the water can be used as a drinking water, with it now being safe for human consumption. Also, industrial operations may result in trace levels of valuable inorganic metal forms being left in the water used in the process. An example of this would be small residuals of silver nitrate from photographic emulsion processes.

Currently, ion-exchange is the most commonly used high purity water process for removing trace levels of inorganic impurities from water. Ion exchange resins are synthetic polymers consisting of styrene that is cross-linked with divinylbenzene.[161] A cation exchange resin is used to remove positively charged ions from water and an anion exchange resin is used to remove negatively charged ions. For cation resins, the resin is treated with a strong mineral acid (hydrochloric or sulfuric) which leaves hydrogen as the

functional group. Similarly, an anion resin is treated with a strong base such as sodium hydroxide, leaving hydroxyl ion as the functional group.

As water is passed through the resin, the cation resin will remove cationic species such as sodium, potassium, magnesium, barium, and replace these in the water stream with hydrogen. The anion resin will remove anionic ions such as chloride, sulfate, dichromate, nitrate and replace with these hydroxyl ion. The net result is that an anionic and a cationic impurity have been removed from the water and replaced with OH-H. The resins can be regenerated again with acid and base, removing the inorganic impurities from the resin and the impurities will now be in a much more concentrated form in a smaller volume of water.

There are several downsides to ion-exchange. It is a chemically energy intensive process due to the high use of regenerant chemicals. These chemicals are hazardous in some form or another, and the regenerants are not used stoichiometrically in the regeneration process, typically 50-100 regenerant ions are needed to regenerate one ion exchange site. Therefore large amounts of strong acid or strong base regenerant are left as waste products.

In comparison, if MD were to be used for the removal of low levels of inorganic impurities from water it would require an energy input for fabrication, but would not require the use of regenerant chemicals nor would hazardous waste be produced.

6.2 Experimental Section

Two new modules, the same as those previously used were prepared. Six compounds were tested in this study: sodium chloride, magnesium chloride, magnesium sulfate, barium chloride, silver nitrate and potassium dichromate. Solutions of each were prepared in ultrapure deionized water (supplied by Mr. S. Vetrano of Graver

Technologies, Newark, NJ, USA). Conductivity analysis of the feed, permeate and concentrate solutions were completed. Each experiment was completed in triplicate and each sample was analyzed three times. Deionized water controls were analyzed with each experiment.

6.3 Results and Discussion

Membrane performance was determined by two measures. First, the ratio of the concentration of the chemical of interest in the final concentrate to the concentration in the feed solution is referred to as the Enrichment Factor (EF):

$$EF = \left(\frac{C_c}{C_f} \right) \tag{6.1}$$

where C_c is the concentration in the concentrate stream and C_f is the concentration in the feedwater stream.

Second, the reduction in feed water volume (SR) is defined as:

$$\%SR = \frac{V_{f-}V_c}{V_f} X100 \tag{6.2}$$

where V_f and V_c are the feed solution and concentrate volumes.

Process optimization experiments for temperature, feed flow rate and sweep air temperature were conducted using a 10 mg L^{-1} NaCl solution. Experiments where the feed solution temperature was varied showed maximum enrichment occurred when the aqueous feed solution was 80ºC for both membranes. Results for this are shown in

Figure 6.1. As expected, there was a distinct temperature effect, with both EF and %SR increasing with temperature up to about 80ºC and then decreasing at higher temperature. Significantly, the CNIM had 3-4 times the amount of enrichment and volume reduction than did the plain membrane at all temperature points. In fact the CNIM's solvent reduction at 60ºC was 400% higher than the plain membrane's highest reduction at 80ºC. Similarly the CNIM had 200% more concentrate enrichment than did the plain membrane at the same temperatures. This demonstrates the CNIM performs better with a much lower energy input.

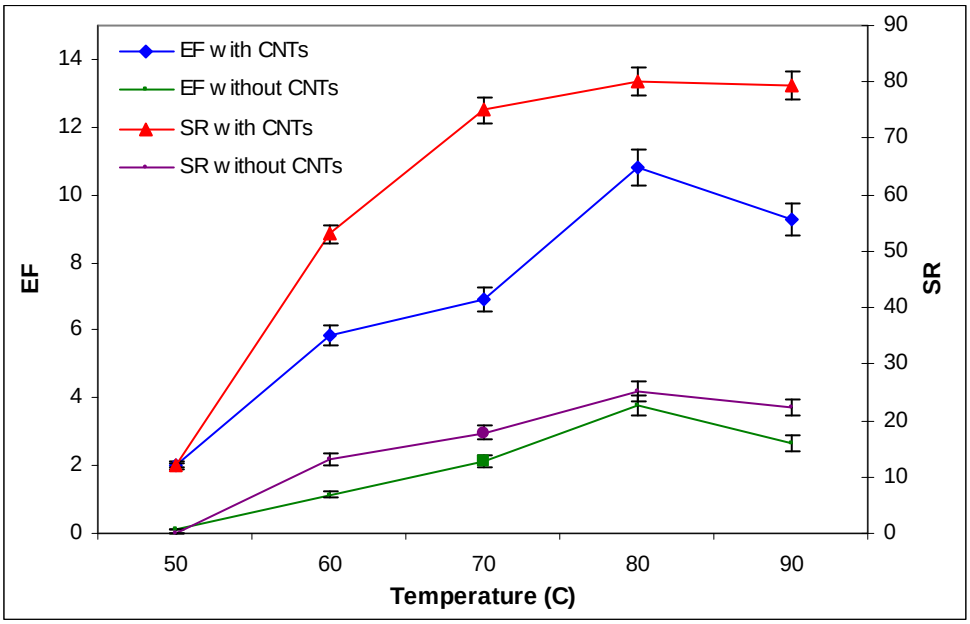

Figure 6.1 Concentrate enrichment and reduction in feed water volume as a function of temperature at 0.75 ml min^{-1}.

The mass transfer coefficients at different temperatures are presented in Figure 6.2, and were found to be up to 6 times higher in the presence of the CNTs at 60°C and approximately 2 times greater at higher temperatures. This highlights the greater overall energy efficiency of the CNIM at lower temperatures.

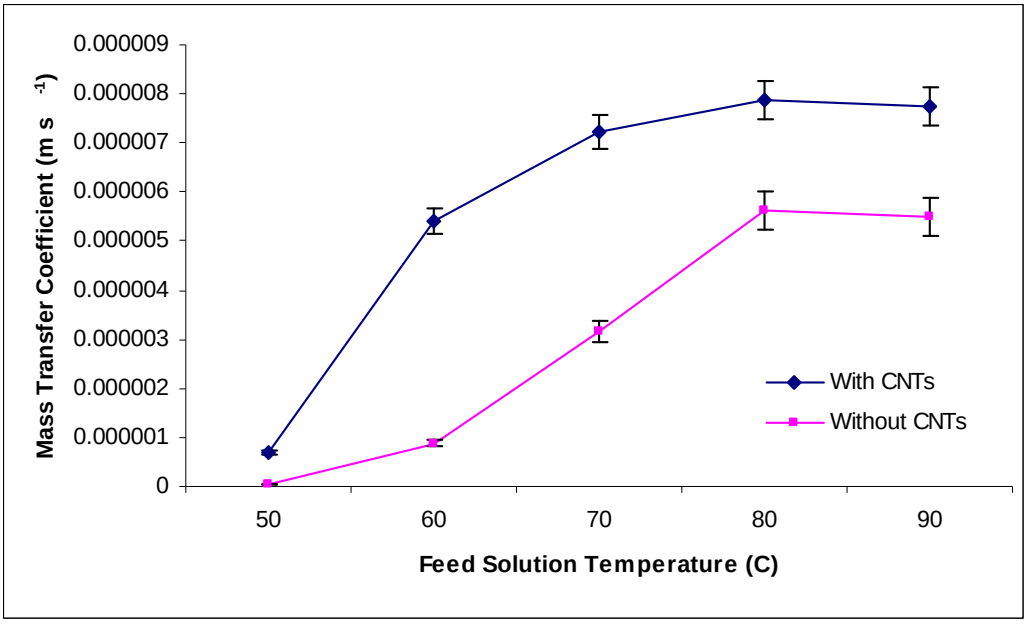

Figure 6.2 Mass transfer coefficient (m/s^{-1}) as a function of temperature.

Results for feed solution flow rates are shown in Figure 6.3. Optimal enrichment occurred at 0.75 ml min^{-1} feed flow rate for both membranes. The CNIM was higher than the plain membrane at all flows and the CE and %RV for the CNIM at the highest flow were respectively about 200% and 350% higher than for the plain membrane at the optimal flow rate. Again, this indicates a much lower energy requirement is needed for the CNIM to obtain the same results.

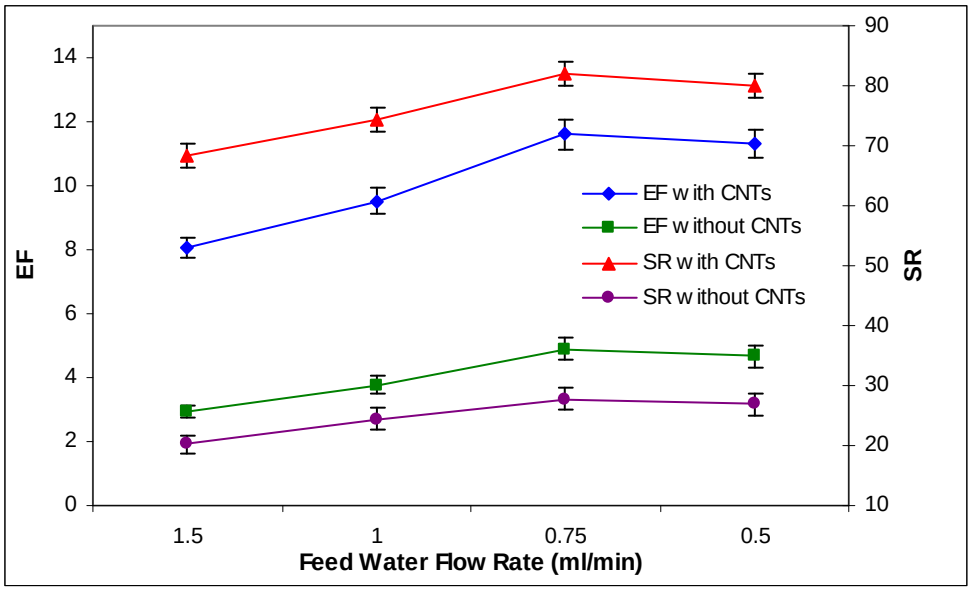

Figure 6.3 Concentrate enrichment and reduction in feed water volume as a function of flow rate at 80°C.

Figure 6.4 shows the effect of flow rate on the mass transfer coefficient. The profile for the unmodified membrane was much flatter than the CNIM and mass transfer coefficients were about 3.3 times higher for the CNIM at all flow rates.

Several authors [162-163] have reported enhanced MD effects using sweep air across the membranes to help aid in the removal of condensed permeate. Experiments were conducted at 20, 30 and 40ºC sweep air temperature. Results are shown in Figure 6.5 and only indicate a minor improvement with increasing sweep air temperature.

All further experiments were conducted at a feed flow of 0.75 ml min^{-1}, a feed solution temperature of 80ºC and 40ºC sweep air. For each compound, concentration and water reduction effects were measured at feed solutions of 10.0, 1.0 and 0.1 mg L^{-1}, results are summarized in Tables 6.1 and 6.2. For all compounds tested, the EF was 2 to 3 times higher and the %SR was up to 65% greater for the CNIM than for the plain membrane.

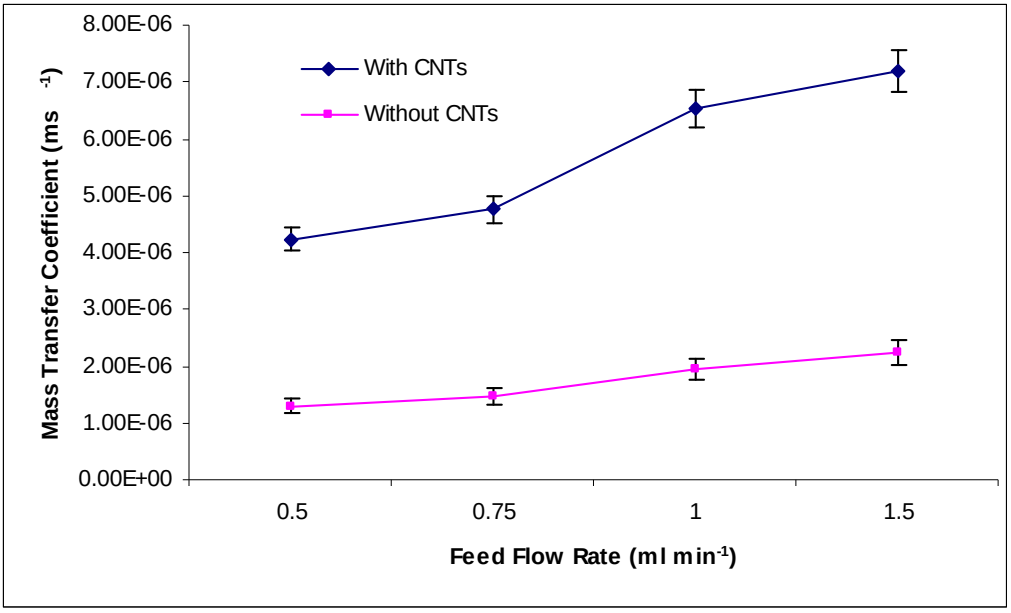

Figure 6.4 Mass transfer coefficient (m/s^{-1}) as a function of feed flow rate.

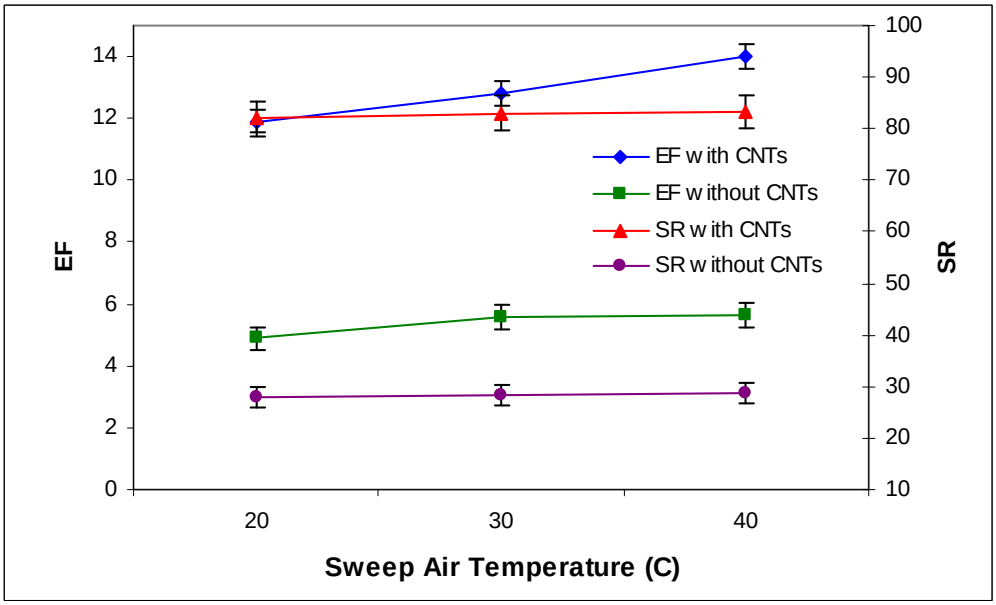

Figure 6.5 Sweep air temperature effects on concentrate enrichment and reduction in feed water volume sweep air effects, 10 mg L^{-1} NaCl Feed solution, 80ºC. Feed solution temperature, 0.75 ml min^{-1} feed rate.

6.4 Conclusions

The presence of CNTs in a hydrophobic membrane pore's allowed for greater enrichment and solvent reduction than did membranes without CNTs. Concentrate enrichment increased by up to a factor of 3 and the reduction in feed water volume increased by as much as 64%. Work completed demonstrated that enhanced membrane distillation using CNTs allows for significantly more enrichment of trace inorganic compounds in aqueous streams. The presence of CNTs likely increased enrichment and solvent reduction by more effective thermal conductance, lower temperature polarization and less pore wetting. The low energy requirements of this process makes it an attractive alternative for applications to either remove toxic inorganic impurities or to recover valuable product.

Table 6.1 Enrichment Factor (EF) for Six Compounds at 10.0, 1.0 and 0.1 mg L^{-1} Feed Solution with Plain Membranes and with CNIM. Feed flow 0.75 ml min-1, 80°C and 40°C Sweep Air

	EF With CNTs			EF Without CNTs		
Feed Solution Concentration (mg L^{-1})	**10.0**	**1.0**	**0.1**	**10.0**	**1.0**	**0.1**
NaCl	14	16	20	6	7	10
$MgCl_2$	14	18	25	6	6	11
$MGSO_4$	13	18	25	5	9	13
$BaCl_2$	15	18	24	5	7	12
$AgNO_3$	18	21	22	6	8	13
$K_2Cr_2O_7$	15	17	23	5	7	11

Table 6.2 Solvent (%SR) for Six Compounds at 10.0, 1 and 0.1 mg L^{-1} Feed Solution with Plain Membranes and with CNIM. Feed flow 0.75 ml min^{-1}, 80°C and 40°C Sweep Air

	%SR With CNTs			% SR Without CNTs		
Feed Solution Concentration (mg L^{-1})	**10.0**	**1.0**	**0.1**	**10.0**	**1.0**	**0.1**
NaCl	83	80	85	29	36	38
$MgCl_2$	86	88	85	32	34	33
$MGSO_4$	88	89	89	27	29	29
$BaCl_2$	87	88	88	27	24	25
$AgNO_3$	85	87	86	30	29	29
$K_2Cr_2O_7$	87	88	88	26	27	30

REFERENCES

1. Mitra, S., Sample preparation techniques in analytical chemistry. John Wiley & Sons, Inc.; Hoboken, New Jersey, **2003.**

2. Kataoka, H,; Ishizaki,; A.; Saito, K., Developments and applications of capillary microextraction techniques: A review. *Anal. Chem. Acta.* **2009**, *655*, 8-29.

3. Mulder, Marcel. Basic Principles of Membrane Technology. Kluwer Academic Publishers,. Dordrecht, Ger. **1991**.

4. Li, N. N.; Strathmann, H., Separation Technology: Proceedings of the Engineering Foundation Conference, New York. **1988.**

5. Madden, A.J.; Hayward,M.J., Sheet materials for use as membranes in membrane introduction mass spectrometry. *Anal Chem.* **1996**, *68*, 1805-1811.

6. Liu, R.; Qiao, X.; Chung, T-S., In-line formation of chemically cross-linked P84® co-polyamide hollow fiber membranes for H_2/CO_2 separation *Chem. Eng. Sci.* **2005**, *60*, 6674-6686.

7. Thompson, A.J.; Etzkorn, J.M.; Van Pel,D.; Krogh, E.T.; Drakeford, D.M.; Gill**,** C.G**,** Membrane introduction tandem mass spectrometry (MIMS-MS/MS) as a real-time monitor for biogenic volatile organic compound (BVOC) emissions from plants. *Can. J. Anal. Sci. & Spectro*. **2008**, *53*, 75-81.

8. Bauer, S.; Graham-Cooks, R., Performance of an ion trap mass spectrometer modified to accept a direct insertion membrane probe in analysis of low level pollutants in water *Talanta* **1993**, *40*,1031-1039.

9. Milagre, C. D. F.; Milagre, H. M. S.; Rodrigues, J. A. R.; Rocha, L. L.; Santos, L.S.;Eberlin, M. N., On-line Monitoring of bioreductions via membrane introduction mass spectrometry *Biotech. & Bioeng.* **2005***, 90,* 888-892**.**

10. Cotte-Rodríguez, I.; Handberg, E.; Noll,R.J.; Kilgour D.P.A.; Cooks. R.G., Improved detection of low vapor pressure compounds in air by serial combination of single sided membrane introduction with fiber introduction mass spectrometry. *Analyst* **2005**, *130*, 679-686.

11. Guo,X; Mitra, S.,. Development of membrane purge and trap for measurement of volatile organics in water. *Anal.Lett.* **1998***, 31,* 367-379**.**

12. Xu, Y.H.; Mitra, S., Continuous monitoring of volatile organic compounds in water using online extraction and microtrap gas chromatography system. *J. Chromatogr*. *A* **1994,** *688,*171-180.

13. San Juan, A.; Guo, X.; Mitra, S., On-site and on-line analysis of chlorinated solvents in groundwater using pulse introduction membrane extraction gas chromatography. *J. Sep. Sci.* **2001**, *24,* 599-605.

14. Kou, D.; San Juan, A.; Mitra, S., Gas injection membrane extraction for fast on-line analysis using GC detection. *Anal. Chem*. **2001**, *73,* 5462-5467.

15. Kou, D.; Mita, S., Simultaneous extraction and concentration by on-line hollow fiber membrane extraction. *Anal. Chem*. **2003**, *75*, 6355-6360.

16. Wang, X.; Saridara, C.; Mitra, S., microfluidic supported liquid membrane extraction. *Anal. Chim. Acta.,* **2005**, *543*, 92-98.

17. Hylton, K.; Sangwan, M., Mitra, S.; Microscale membrane extraction of diverse antibiotics from water. *Anal. Chim. Acta.,* **2009**, *653*, 116-120.

18. Hylton, K.; Chen, Y.; Mitra, S. Automated, on-line membrane extraction. *J. Chromatogr. A* **2007**, *1152*, 199-.214.

19. Bishop, EJ.; Mitra, S, Measurement of nitropheols in air samples by impinger sampling and supported liquid membrane micro-extraction. *Anal. Chim. Acta* **2007**, *583*, 10-14.

20. Wang, X.; Kou, D.; Mitra, S., Continuous on-line monitoring of haloacetic acids via membrane extraction. *J. Chromatgr. A* **2005**, *1089*, 39-44.

21. Hylton, K.; Mitra, S., Barrier film protected and mixed solvent optimized micro-scale membrane extraction of methyl carbamate pesticides. *J. Chromatogr. A* 2007, *1154*, 60-65.

22. Hylton, K.; Mitra, S., A microfluidic hollow fiber membrane extractor for arsenic (V) detection. *Anal. Chim. Acta*. **2008**, *607*, 45-49.

23. Kou, D.; Wang, X.; Mitra, S., Supported liquid membrane extraction with high performance liquid chromatography-UV detection for monitoring trace haloacetic acids in water. *J. Chromatogr. A* **2004**, *1055*, 63-69.

24. Wang, X.; Mitra, S., development of a total analytical system by interfacing membrane extraction, pervaporation and high performance liquid chromatography. *J. Chromatogr. A* **2005**, *1069*, 237-242.

25. Jung , L.; Chimuka, J.-Å.; Jönsson , N.; Niedack, P.; Bowens; Alsanius B., Supported liquid membrane extraction for identification of phenolic compounds in the nutrient solution of closed hydroponic growing systems for tomato *Anal. Chim. Acta* **2002**, *474*, 49-57.

26. McMurray, S.H.; Griffin, G.J., Extraction of aconitic acid from mixtures of organic acids and cane molasses solutions using supported liquid membranes. *J Chem. Technol. Biotechnol.* **2002**, *77*, 1262-1268.

27. Rasmussen, K.E.; Pedersen-Bjergaard, S., *Trends Anal. Chem*. **2004,** *23*, 521-523.

28. Barri, S.; Bergstrom, Norberg, J.; Jonsson, J.A., Miniaturized and automated sample pretreatment for determination of PCBs in environmental aqueous samples using an on-line microporous membrane liquid-liquid extraction-gas chromatography system. *Anal. Chem.* **2004,** *76*, 1928-1934.

29. Basheer, C.; Lee, H.K., Hollow fiber membrane protected solid-phase micro-extraction of tirazine herbicides in bovine milk and sewage sludge samples. *J. Chromatogr. A* **2004**, *1047*, 189-194.

30. Jonsson, A.; Mathiasson. L., Liquid membrane extraction in analytical sample preparation: II. Applications . *TrAC Trends in Anal. Chem.* **1999,** *4***,** 325-334.

31. Luo, Y.Z.; Pawliszyn, J., Membrane extraction with a sorbent interface for headspace monitoring of aqueous samples using a cap sampling device. *Anal. Chem.,* **2000**, *72*, 1058-1063.

32. Allen, T.M.; Falconer, T.; Cisper, M.E.; Bergerding, A.J.; Wilkerson, C.W., Real-time analysis of methanol in air and water by membrane introduction mass spectrometry. *Anal. Chem.,* **2001**, *73*, 4830-4835.

33. Thompson, A.J.; Creba, A.S.; Ferguson, R.M.; Krogh, E.T.; Gill, C.G., A coaxially heated membrane introduction mass spectrometry interface for the rapid and sensitive on-line measurement of volatile and semi-volatile organic contaminants in air and water at parts-per-trillion levels. *Rapid Commun. Mass Spectrom*. **2006**, *20*, 2000-2008.

34. Audunsson, G., Aqueous/aqueous extraction by means of a liquid membrane for sample cleanup and preconcentration of amines in a flow system. *Anal. Chem*. **1986,** *58*, 2714-2723.

35. Castro, M.D.L.; Gamiz-Gracia, L., Analytical pervaporation: an advantageous alternative to headspace and purge and trap techniques. *Chromatographia* **2000**, *52,* 265-272.

36. Reyes, F.D.; Romero, J.M.F.; Castro, M.D.L., Selective inhibition-based biosensing system for the determination of pesticides in environmental samples using analytical pervaporation coupled with enzymatic derivitization. *Anal*. *Chim. Acta.* **2000***, 408*, 209-216.

37. Panek, D.; Konieczny, K., Pervaporative separation of toluene from wastewater by use of filled and unfilled poly(dimethylosiloxane) (PDMS) membranes. *Desal.* **2009**, *24,* 197-200.

38. Papaefstathiou, I.; Castro, M.D.L.,Hyphenated pervaporation-solid-phase preconcentration gas chromatography for the determination of volatile organic compounds in sold samples. *J. Chromatogr. A* **1997**, *779*, 352-359.

39. Peeraprasompong, P.; Thavarungkul, P.; Kanatharana, P., Development of an in-line system for the analysis of 4-4'-DDT in water. *J. Environ. Sci. Heal. B* **2006**, *41* 807-819.

40. Vallejo, B.; Richter, P.; Toral, I.; Tapia, C.; Castro, M.D.L., Determination of sulfide in liquid and solid samples by integrated pervaporation-potentiometric detection. *Anal. Chim. Acta.* **2001**, *436,* 301-307.

41. Papaefstathiou, I.; Castro, M.D.L., Integrated pervaporation/detection:continuous and discontinuous approaches for treatment/determination of fluoride in liquid and solid samples. *Anal. Chem.* **1995,** *67*, 3916-3921.

42. Rupasinghe, T.; Cardwell,T.J.; Cattrall,R.W.; Potter, I.D.; Kolev, S.D. Determination of arsenic by pervaporation-flow injection hydride generation and permanganate spectrophotometric detection. *Anal. Chim. Acta* (**2004**), *510*, 225-229.

43. Caballo-Lopez, A.; Castro, M.D.L., Hydride generation-pervaporation-atomic fluorescence detection prior to speciation analysis of arsenic in dirty samples. *J. Anal. At. Spectrom.* **2002** *17*, 1363-1367.

44. Maden, A.J.; Hayward, M.J., Sheet materials for use as membranes in membrane introduction mass spectrometry. *Anal. Chem.* **1996**, *68,* 1805-1811.

45. Bryce, D.W.; Izquierdo, A.; Castro, M.D.L., Pervaporation as an alternative to headspace. *Anal. Chem.* **1997,** *69*, 844-847.

46. Ruiz-Jimenez, J.; Castro, M.D.L., Pervaporation as interface between solid samples and capillary electrophoresis: determination of biogenic amines in food. *J. Chromatogr. A* **2006**, *1110***,** 245-253.

47. Wang, X.; Mitra, S., Development of a total analytical system by interfacing membrane extraction, pervaporation and high-performance liquid chromatography. *J. Chromatogr. A* **2005,** *1068*, 237-242.

48. Cañizares, P.; Castro, M.D.L., Enzymatic interface-free assay for oxylate in urine. *J. Anal. Chem*. **1997**, *357*, 777-781.

49. Nacapricha, D.; Sangkarn, P.; Karuwan, C.; Mantima, T.; Waiyawat, W.; Wilairat, P.; Cardwell,; T.; McKelvie, I.D.; Ratanawimarnwong, N., Pervaporation-flow injection with chemiluminescence detection for determination of iodide in multivitamin tablets. *Talanta* **2007**, *72,* 626-633.

50. Gamiz-Gracia, L.; Castro, M.D.L., Integrated pervaporation detection for the determination of fluoride in pharmaceuticals. *J. Pharm. Biomed. Anal*. **2000**, *22*, 909-913.

51. Gomez-Ariza, J.L.; Garcıa-Barrera, T.; Lorenzo, F., Analysis of anisoles in wines using pervaporation coupled to gas-chromatography-mass spectrometry. .*J. Chromatogr. A* **2004**, *1049*, 147-153.

52. Gomez-Ariza, J.L.; Garcıa-Barrera, T.; Lorenzo, F., Determination of flavor and off-flavor compounds in orange juice by on-line coupling of a pervaporation unit to gas-chromatography-mass spectrometry. *J. Chromatogr. A* **2004**, *1047*, 313-317.

53. Ruiz-Jimenez, J.; Castro,M.D.L., On-line pervaporation-capillary electrophoresis for the determination of volatile analytes in food slurries. *J. Chromatogr. A* **2006**, *1128,* 251-258.

54. Sae-Khow. O.; Mitra, S., Simultaneous extraction and concentration in carbon nanotube immobilized hollow fiber membranes. *Anal. Chem*. **2010**, *82*, 5561-5567.

55. Garcıa-Garrido, J.A.; Castro, M.D.L., Determination of trimethylamine in fish by pervaporation and photometric detection. *Analyst* **1997**, *122*, 663-666.

56. Shao, P.; Huang, R.Y.M., Polymeric membrane pervaporation. *J. Membr. Sci.* **2007**, *287*, 162-179.

57. Peng, M.; Vane, L.M.; Liu, S.X., Recent advances in VOC removal from water by pervaporation. *J. Hazard. Mater.* **2003**, *98,* 69-90.

58. Smitha, B.; Suhanya, D.; Sridhar, S.; Ramakrishna, M., Separation of organic-organic mixtures by pervaporation- a review. *J. Membr. Sci.* **2004***, 241,* 1-21.

59. Dutta, B.K.; Sikdar, S.K., Separation of volatile organic compounds from aqueous solutions by pervaporation using S-B-S block copolymer membranes. *Environ. Sci. Technol*. **1999**, *33*, 1709-1716.

60. Polotskaya, G.A., Penkova, A.V., Toikka, A.M.; Fullerene-containing polyphenylene oxide membranes for pervaporation. *Desal.* (**2006**), *200*, 400-402.

61. Bishop, E.; Mitra, S., Hollow fiber membrane concentrator for on-line preconcentration. *J. Chromatogr. A* **2004**, *1046*, 11-17.

62. Bishop, E.; Mitra, S. On-line membrane preconcentration for continuous monitoring of trace pharmaceuticals. *J. Pharma. Biomed Anal.* **2005,** *37,* 81-86.

63. Khayet, M; Godino M.P.; Mengual, J.I.; Theoretcial and experimental studies on desalination using the sweeping gas membrane distillation method. *Desal.* **2003**, *157*, 297-305.

64. Evans, L.R.; Miller, J.E. Sandia National Laboratories, Sweeping Gas Membrane Desalination Using Commercial Hydrophobic Hollow Fiber Membranes SAND REPORT, **2002-0138.**

65. Drioli, E.; Calabro V.; Wu, *Y.* Microporous membranes in membrane distillation. *Pure & Applied Chem.* **1986**, *58*, 1657-1672.

66. Curcio, E., Drioli, E.; Membrane distillation and related operations- a review. *Sep. and Pur. Rev.,* **2005**, *34*, 35-86.

67. Baumeister, T., Mark's Standard Handbook for Mechanical Engineers, Eighth Edition McGraw-Hill Book Company, **1978** Ch. 4.

68. Sirkar, K.K.; Li, B., New Jersey Institute of Technology, Novel Membrane and Device for Direct Contact Membrane Distillation-Based Desalination Process, US-Department of the Interior Agreement 01-FC-81-0737, Report 96, **2003.**

69. Bausa, J.; Marquardt, W., Shortcut design methods for hybrid membrane distillation processes for the separation of nonideal multicomponent mixtures. *Ind. Eng. Chem. Res.* **2000**, *39*, 1658-1672.

70. Izquierdo-Gil, M.A.; Fernandez-Pineda, C.; Lorenz, M.G., Flow rate influence on direct contact membrane distillation experiments: different empirical correlations for Nuselt number. *J. Membr. Sci.* **2008**, 321, 356-363.

71. Tomaszewska, M., Membrane distillation examples of applications in technology and environmental protection. *Polish J. Env. Stud*. **2000**, *9*, 27-36.

72. Rivier, C., Garcia-Payo, M.; Marisol, I.; von Stockar, U., Separation of binary mixtures by thermostatic sweeping gas membrane distillation I. theory and simulations. *J. Memb. Sci*. **2002**, *201*, 1-16.

.

73. Xu, J.; Furuswa, M.; Ito, A., Air-sweep vacuum membrane distillation using fine silicone rubber, hollow fiber membranes. *Desal*. **2006**, *191*, 223-231.

74. Peng, P.; Fane, A.G.; Li, X.,; desalination by membrane distillation, adopting a hydrophilic membrane. *Desal*. **2005**, *173*, 45-54.

75. Banat, F.; Al-Rub, F.A.; Shannag, M., Modeling of dilute ethanol-water mixture separation by membrane distillation. *Sep. & Pur. Tech*. **1999**, *16*, 119-131.

76. College of Engineering, University of Texas at El Paso, Solar and Waste Heat Desalination by Membrane Distillation, Program Report No. 8, **2004**.

77. Cath,T.Y.; Adams,V.; Childress, A.E., Experimental study of desalination using direct contact membrane distillation: a new approach to flux enhancement. *J. Membr. Sci*. **2004**, *228,* 5-11.

78. Cabassud, C., Wirth, D.; Membrane distillation for water desalination: how to choose an appropriate membrane. *Desal*. **2003,** *157,* 307-313.

79. Galvez, J.; Garcia-Rodriguez, L.; Martin-Mateos, I., Seawater desalination by an innovative solar-powered membrane distillation system: the MEDESOL project. *Desal*. **2009**, *246*, 567-576.

80. Ji., X.; Curcio, E.; Al-obaidani, S.; DiProfio, G.; Fontanova, E.; Drioli, E., Membrane distillation- crystallization of seawater reverse osmosis brines. *Pur, Tech. 2010*, *71*, 76-82.

81. Song. L.; Baoan, L.; Sirkar, K.; Gilron, J., Direct contact membrane distillation-based desalination: novel membranes, devices, larger-scale studies and a model. *Ind. Eng. Chem. Res.* **2007**, *46*, 2307-2323.

82. Alklaibi, A.; Lior, N., Membrane-distillaiton desalination: status and potential. *Desal*. **2004**, *171*, 111-131.

83. Martinez-Diez, L.; Florido-Diaz, F.; Vasquez-Gonzalez, M.I., Study of evaporation efficiency in membrane distillation. *Desal*. **1999**, *1276*, 193-198.

84. Gunko, S.: Vrbych, S.: Bryk, N., Concentraion of apple juice using direct contact membrane distillation. *Desal*. **2006**, *190,* 117-124.

85. Ding, Z.; Liu, L.; Yu, J.; Ma, R.; Yang, Z., Concentrating the extract of traditional chinese medicine by direct contact membrane distillation. *J. Membr. Sci.* **2008**, *310*, 539-549.

86. Christensen, K.; Andresen, R.; Tandskov, I.; Nordahl, B.; du Preez, J., Using direct contact membrane distillation for whey concentration. *Desal*. **2006**, *200*, 523-525.

87. El-Bourawi, M.S.; Kyayet, M.; Ding, Z.; Li, Z.; Zhang, X., Application of vacuum membrane distillation for ammonia removal. *J. Membr. Sci*. **2007**, *301*, 200-209/

88. Yun, C.; Prasad, R.; Guha, A.; Sirkar, K., Hollow fiber solvent extraction removal of toxic heavy metals from aqueous waste streams. *Ind. Eng. Chem. Res.* **1993**, *32*, 1186-1195.

89. Cassano, A.; Drioli, E.; Galaverna, G.; Marchelli, R.; DiSilvestro, D.; Cagnasso, C., Clarification and concentration of citrus and carrot juices by integratred membrane processes. *J.Food Engin*. **2003**, *57,* 153-163.

90. Soni, V.; Abildskov, J.; Jonsson, G.; Gani, R., Modeling and analysis of vacuum membrane distillation for the recovery of volatile aroma compounds from black currant juice. *J. Membr. Sci*. **2008**, *320*, 442-455.

91. Kozak, A.; Rektor, A.; Vatai, G.; Production of black currant juice by using membrane disgtillation. *Desal*. **2008**, *200*, 540.

92. Nene, S.; Kaur, S.; Sumod, K.; Joshi, B.; Raghavarao, K., Membrane distillation of raw-cane sugar syrup and membrane clarified sugarcane juice. *Desal*. **2002**, *147*, 157-160.

93. Pontius, F., Editor- Water Quality and Treatment, AWWA, Fourth Edition, McGraw-Hill, **1990**, Chp. 11.

94. Martinez, L., Comparison of membrane distillation performance using different feeds. *Desal*. **2004**, *168*, 359-365.

95. Alves, V.D., Coelhoso, I.M.; Effect of membrane characteristics on mass and heat transfer in the osmotic evaporation process. *J. Membr. Sci.* (**2004**), *228*, 159-167.

96. Quinones-Bolanos, E.; Zhou, H.; Soundararajan, R.; Otten, L.; Otten, L., Water and solute transport in pervaporation hydrophillic membranes to reclaim contaminated water for micro-irrigation. *J. Membr. Sci*. **2005**, *252*, 19-28.

97. Hasanoglu, A.; Salt, Y.; Keleser, S.; Ozkan, S.; Dincer, S., Pervaporation separation of organics from multicomponent aqueous mixtures. *Chem. Eng. Proc*. **2007**, *46*, 300-306.

98. Martinez-Diaz, L.; Vazquez-Gonzalez, M.I., A method to evaluate coefficients affecting flux in membrane distillation. *J. Membr. Sci.* **2000**, *173*, 225-234.

99. Deng, S.; Solar Distillation of Brackish Water Using Membrane Distillation Process, WRRI Technical Completion Report No. 342, New Mexico Water Resources Institute. Water Resources Institute. January **2008**.

100. Bandini, S.; Gostoli, C.; Sarti, G.C., Role of heat and mass transfer in membrane distillation process. *Desal*. **1991**, *81*, 91-106.

101. Celere, M.; Gostoli, C., The heat and mass transfer phenomena in osmotic membrane distillation. *Desal*. **2002**, *147*, 133-138.

102. Minnelli, G.; La Aruba, V.; Bruceton, V., Characterization of hydrophobic polymeric membranes for membrane distillation process. *Int. J. Mater. Form.* **2010**, *3*, 563-566.

103. Tasha, M.; Matsuura, T.; Kruse, B.; Khayet, M., Heat and mass transfer analysis in direct contact membrane distillation. *Desal*. 2008, 219, 272-292.

104. Harder, E.; Walters, D.; Bonder, Y.; Fairish, R.; Roux, B., Molecular dynamics of a polymeric reverse osmosis membrane. *J. Phys, Chem. B* **2009**, *113*, 10177-10182.

105. Babur, B.; Restage, O.K.; Raghavarao; K.S., Concentration and temperature polarization effects during osmotic membrane distillation. *J. Membr. Sci.* **2008** *322*, 146-153.

106. Scherer, J.; Bolton, B., Water in polymer membranes, on the existence of pores and voids. *J. Phs. Chem*. **1985**, *89*, 3535-3540.

107. Diban, N.; Voinea, O.; Urtiaga, A.; Ortiz, I., Vacuum membrane distillation of the main pear aroma compound: experimental study and mass transfer modeling. *J. Membr. Sci*. **2009**, *326*, 64-75.

108. Pangarkar, B.L.; Parjane, S.B.; Abhanng, R.M.; Guddad, M., *Int. J. Chem. & Bio. Eng*. **2010**, *3*, 33-38.

109. Caballo-Lopez, A.; Castro, M.D.L., Continuous ultrasound assisted extraction coupled to flow injection pervaporation, derivitization and spectrophotometric detection for the detection of ammonia in cigarettes. *Anal. Chem.* **2006**, *78*, 2297-2301.

110. Gethard, K.; Mitra, S., Membrane distillation as an on-line concentration technique: application to the determination of pharmaceutical residues in natural waters. *Anal. Bioanal. Chem.* **2011**, 400,571-575.

111. Vandeford, B.J.; Snyder, S.A., Analysis of Pharmaceuticals in Water by Isotope Dilution Liquid Chromatography/Tandem Mass Spectrometry. *Environ. Sci. Technol.* **2006**, *40*, 7312-7320.

112. Baoan, L; Sirkar, K.K., Novel membrane and device for vacuum membrane distillation based distillation process. *J. Membrane Sci*. **2004** *257*, 60-75.

113. Baranowska, I.; Kowalski, B., The development of SPE procedures and an UHPLC method for the simultaneous determination of ten drugs in water samples *Water, Air, Soil Poll*. **2010**, *211*, 417-425.

114. Guide to Inspections- Validation of Cleaning Processes U.S. Department of Health and Human Services, Food and Drug Administration January **2006.**

115. PAT- A Framework for Innovative Pharmaceutical Development, Manufacturing and Quality Assurance U.S. Department of Health and Human Services, Food and Drug Administration September **2004**.

116. Wiesler, F.; Sodaro, R., Degasification of water using novel membrane technology. *Ultrapure Water* **1996**, *UP130653*, 53-56.

117. Wiesler, F., Membrane contactors: an introduction to the technology. *Ultrapure Water* **1996**, *UP-1304427*, 27-31.

118. USP Monographs for Ibuprofen, Dibucaine Hydrochloride and Diphenhydramine USP 31-NF26, **2006**.

119. Marin, A.; Garcia, A.; Barbas, C., Validation of a HPLC quantification of acetaminophen, phenylephrine and chlorpheniramine in pharmaceutical formulations. *J. Pharm. Biomed. Anal*. **2002**, *29*, 701-714.

120. Caballo-Lopez, A.; Castro, M.D.L., Determination of campum in leaves by ultrasound assisted extraction prior to hydride generation, pervaporation and atomic absorption detection. *Talanta* **2007**, *71*, 2074-2079.

121. Al-Obaidani, S.; Curcio, E.; Macedonio, F.; Di Profio; G., Al-Hinal, H.; Drioli, E., Potential of membrane distillation in seawater desalination: thermal efficiency, sensitivity and cost estimation. *J. Membr. Sci.* **2008,** *323,* 85-98.

122. U.S. Environmental Protection Agency, Environmental Monitoring Systems Laboratory, Method 200.2, Revision 2.8.

123. Ericsson, M.D.; Giguere, M.T.; Whitaker, D., An evaluation and comparison of micro-techniques for concentration of volatile components from dilute solutions *Anal. Ltr*. **1981**, *14*, 841-845.

124. Sae-Khow; O., Mitra, S., Carbon nanotubes as the sorbent for integrating u-solid phase extraction within the needle of a syringe. *J. Chromatogr*. *A* **2009**, *1216*, 2270-2274.

125. Sae-Khow, O.; Mitra, S., Fabrication and characterization of carbon nanotubes immobilized in porous polymeric membranes. *J. Mater. Chem.* **2009**, *19*, 3713-3718.

126. Hussain, C.; Saridara, C.; Mitra, S.; Microtrapping characteristics of single and multiwall nanotubes. *J. Chromatogr*. *A* **2009**, *1185*, 161-166.

127. Sae-Khow, O; Mitra, S., Carbon nanotube immobilized composite hollow fiber membranes for pervaporative removal of volatile organics from water. *J. Phys. Chem. C* **2010**, *114*, 16351-16356.

128. Trojanowicz, M., Analytical applications of carbon nanotubes, a review. *TrAc Trends in Anal. Chem*. **2006**, *25*, 480-489.

129. Striolo, A., The mechanism of water diffusion in narrow carbon nanotubes. *Nano Lett*. **2006**, *6*, 633-630.

130. Hummer, G.; Rasaiah, J.C.; Noworta, J.P., Water conduction through the hydrophobic channel of a carbon nanotube. *Nature* **2001**, *414*, 188-190.

131. Thomas, G.A.; McGaughey, A.J.H., Reassessing Fast Water Transport through Carbon Nanotubes. *Nano Lett*, **2008**, *8*, 2788-2793.

132. Dehouche, Z.; Lafi, L.; Grimard, N.; Goyette, J.; Chahine, R., The catalytic effect of single-wall carbon nanotubes on the hydrogen sorption properties of sodium alanates *Nanotech*. **2005**, *16*, 402- 409.

133. Kalra, A.; Garde, S.; Hummer, G., Osmotic water transport through carbon nanotube membranes. *PNAS* June 3, **2003**

134. Popov, V.N., Carbon nanotubes: properties and application. *Mater. Sci. & Eng*. **2004**, *43*, 61-102.

135. Hone, J.; Whitney, M.; Piskotti, C.; Zettl, A., Thermal conductivity of single walled carbon nanotubes. *Phys. Rev. B* **1999**, *59*, 2514-2516.

136. Albo, S.; Broadbelt, L.; Snurr, R., Multiscale modeling of transport and residence times in nanostructured materials. *AIChE J*. **2006**, *52*, 3679-3687.

137. Zhang, Y.; Wang, Z.; Jiang, W., A sensitive fluorimetric biosensor for detection of DNA hybridization based on Fe/Au core/shell nanoparticles. *Analyst* **2011**, *136*, 702-707.

138. Holt, J.K.; Park, H.G.; Wang, Y.; Stadermann, M.; Artyukhin, A.B.; Grigoropoulos, C.P.; Noy, A.; Bakajin, O., Fast mass transport through sub-2 nanometer carbon nanotubes. *Science* **2006**, *312*, 1034-1037.

139. Al-Asheh, S.; Banat, F.; Qtaishat, M.A., Concentration of sucrose solutions via vacuum membrane distillation. *Desal*. **2006**, *195*, 60-68.

140. Pawliszn, J., Sample preparation, quo vadis? *Anal. Chem.* **2003**, *75*, 2543-2558.

141. Nan, W.; Shi Z.; Lin, Y., A simple model for thermal conductivity of carbon nanotube based composites. *Chem. Phy. Ltrs*. **2003**, *375*, 666-669.

142. McElroy, J.P., Surface tension and its effect on vapor pressure. *J. Colloid Inter. Sci.* **1979**, *72*, 147-149

143. Karkare, M.; Fort, T., Water movement in unsaturated porous media due to pore size and surface tension induced capillary pressure gradients. *Langmuir* **1993**, *147*, 2398-2403.

144. Vane, L.; Alvarez, F.; Giroux, E., Reduction of concentration polarization in pervaporation using vibrating membrane module. *J. Membr. Sci.* **1999**, *153*, 233-241.

145. Srisurichan, S.; Jiraratananon, R.; Fane, A.J., Mass transfer mechanisms and transport resistances in direct contact membrane distillation process. *J. Membr. Sci*. **2006**, *277*, 186-194.

146. Pangarkar, B.L.; Parjane, S.B.; Abhanng, R.M.; Guddad, M., The heat and mass transfer phenomena in vacuum membrane distillation for desalination. *Inter.J. Chemi. and Biol. Eng*. **2010**, *3*, 33-38.

147. Jamadagni, S.; Godawat, R.; Garde, S. How surface wettability affects the binding, folding and dynamics of hydrophobic polymers at interfaces. *Langmuir* **2009**, *25*, 13092-13099.

148. Dutta, B.K.; Sikdar, S.K., Separation of volatile organic compounds from aqueous solutions by pervaporation using S-B-S block copolymer membranes. *Environ. Sci. Technol*. **1999**, *33*, 1709-1716.

149. Vane, L.M.; Alvarez, F.R.; Mullins, B., Removal of methyl tert-butyl ether from water by pervaporation: bench and pilot scale evaluations. *Environ. Sci. Technol.* **2001**, *35*, 391-397.

150. World Health Organization Guideline for Drinking Water Quality, Third Edition, Volume 1, **2008**.

151. Pontius, F., Editor- Water Quality and Treatment, AWWA, Fourth Edition, McGraw- Hill, **1990**, Chp. 11.

152. Byrne, W., Reverse osmosis a practical guide for industrial users. Tall Oaks Publishing, Littleton, Colorado, **2002**, Second edition.

153. U.S. EPA Summary of Safe Drinking Water Act Regulations U.S.C. **1972**.

154. Gethard, K.; Sae-Khow, O.; Mitra. S., Water desalination using carbon-nanotube enhanced membrane distillation. *ACS Appl. Mater. & Inter*. **2011**, *3*, 110-114.

155. Strathmann, H., Michaels, A.S., Polymer-water interaction and its relation to reverse osmosis desalination efficiency. *Desal*. **1977**, *21*, 195-202.

156. Burgess, J., Ions in solution: basic principals of chemical interactions; Ellis Horwood, Chichester, UK, **1988**, Ch. 4.

157. Zhou,W.; Song, L., Experimental study of water and salt fluxes through reverse osmosis membranes. *Environ. Sci. Technol.* **2005**, *39*, 3382-3387.

158. Meltzer, T., Pharmaceutical Water Systems; Tall Oaks Publishing, Littleton, CO. **1996**, Chp. 9.

159. Voros, N.G.; Maroulis, D.; Marinos-Kouris, D., Salt and water permeability in reverse osmosis membranes. *Desal.* **1996**, *104***,** 141-154.

160. Filmtec membranes- Factors affecting RO membrane performance, *DOW form 609-00055-498XQRP,* **1998.**

161. Owens, D., Practical Principles of Ion Exchange, Tall Oaks Publishing, Littleton, CO **1985**, Ch 2.

162. Lee, C.H.; Hong, W.H., Effect of operating variables on the flux and selectrivity in sweep gas membrane distillation for dilute aqueous isopropanol. *J Memb. Sci,*, **2001**, *188*, 79-86.

163. Xie, Z.; Duong, T.; Hoang, M.; Nguyen, C.; Bolto, B., Ammonia removal by sweep gas membrane distillation. *Water Research* ***2009***, *43*, 1693-169.